THE WATER INSTITUTE OF THE GULF®

Geomorphic Evolution of the Coupled Raccoon Pass and West Belle Pass Barrier Spit, Louisiana

MARK A. KULP, IOANNIS Y. GEORGIOU, JOHN N. KRAMER, AND KAREN L. MARCHAL

Supported by: Coastal Protection and Restoration Authority and the Baton Rouge Area Foundation (SEP)

June 8, 2016

ABOUT THE WATER INSTITUTE OF THE GULF

The Water Institute of the Gulf is a not-for-profit, independent research and technical services resource for resilient coasts and sustainable water systems worldwide. The work of the Institute helps ensure livable communities and a thriving economy and environment. For more information, visit www.thewaterinstitute.org.

.

SUGGESTED CITATION

Kulo, M.A.; Georgiou, I.Y.; Marchal, K.L.; Kramer, J.N.; Adams, A.P.; Fitzgerald, D.M.; Yocum, T.E.; Lebien, J.; and Brown, M. (2015). Geomorphic Evolution of the Coupled Raccoon Pass and West Belle Pass Barrier Spilt, Louisiana. The Water Institute of the Gulf. Supported by the Coastal Protection and Restoration Authority and the Baton Rouge Area Foundation. Baton Rouge, LA.

Preface

Recognizing that sediment is a resource in the coastal zone, one of the main objectives of this study was to establish a framework for assessing sediment availability in coastal systems. Using surface and subsurface data, and through modern observations of hydrodynamics this study determined modern sediment transport pathways that could explain proximal coastal zone deposits. Furthermore, this study developed a conceptual sedimentary framework and budget of the Bayou Lafourche barrier shoreline located between East Timbalier Island and the Miss Lena - Caminada-Moreau headland, including Raccoon Pass, using historic cores, seafloor change analysis and shorelines, and by interpretation of modern processes. The datasets were used to identify dominant lithofacies of the barrier system at the surface and in the shallow subsurface, determined what processes control the distribution of the identified lithofacies to provide information about dominant sediment transport patterns that have historically influenced the barrier island system, or contributed to the evolution of this system during the recent transgression.

Table of Contents

List of Figures

List of Tables

List of Acronyms

Acronym	Term
BICM	Barrier Island Comprehensive Monitoring
CPRA	Coastal Protection and Restoration Authority
CPD	Cycle per Day
CRL	Coastal Research Laboratory
CWPPRA	Coastal Wetlands Planning, Protection and Restoration Act
DOQQ	Digital Orthophoto Quarter Quadrangle
MRDP	Mississippi River Delta Plain
NAIP	National Agriculture Imagery Program
NOAA	National Oceanic and Atmospheric Administration
UNO	University of New Orleans
USEPA	U.S. Environmental Protection Agency
USGS	U.S. Geologic Survey

Acknowledgements

Funding for this project was from The Water Institute's Science and Engineering Program funded by the Coastal Protection and Restoration Authority (CPRA) and the Baton Rouge Area Foundation (BRAF). Darin Lee and Mead Allison provided feedback for location selection and other aspects of the project, and Michael D. Miner provide insightful feedback on early analysis of subsurface data and modern processes. We thank Andrew Adams, Mike Brown and Duncan FitzGerald for field assistance with vibracoring and sediment sampling, and thank Tara Yocum and Jack LeBien for assistance in laboratory sediment analyses and post-processing and analysis of the hydrodynamic data.

Executive Summary

Raccoon Pass is a transgressive, wave-dominated tidal inlet located between East Timbalier Island and the Caminada-Moreau headland. During the past century, the inlet has experienced significant changes in morphology, hydrodynamics, and distribution of sedimentary deposits due to decreased sand availability, an ongoing transgression of the adjacent barriers, and anthropogenic structures. There was a sharp decrease in the longshore contribution of sediment transport to the Timbalier Islands due to the damming of Bayou Lafourche and the construction of the Belle Pass jetties in the early 20th century. This reduction in sediment supply resulted in a landward migration of the flanking barrier, widening of the tidal inlets, and a reduction of sediment bypassing. In 2012, the West Belle Pass Barrier Headland Restoration Project altered this regime by introducing approximately 2.8 million yds^3 of sand to West Belle Pass Barrier Spit. Recent grab-samples and vibracores throughout the inlet complex document numerous 0.25-2.0 m thick subsurface sand accumulations located landward of the inlet in Timbalier Bay. Satellite imagery, shoreline change analysis, and grain size trends document the westward movement of sand from West Belle Pass contributing to the growth of an approximately 1km long spit platform extending into bayward reaches of Raccoon Pass. Along a tidal inlet to back barrier bay transect, near surface sediments contain sand and shell lag in the inlet but transition to sandy-silt and sand in the vicinity of the flood tidal delta and finally to a shelly mud in the bay. The trends is sedimentary deposits derived from vibracore data within Timbalier Bay also confirm the growth and landward extension of the flood-tidal delta. Hydrodynamic field data indicate that the inlet complex is characterized by ebb dominated water surface elevations, but often inlet velocities are flood-dominated suggesting that sand bypassing may be re-initiated. The sand nourishment at West Belle Pass has provided an opportunity to study barrier arc development in the early stage of Louisiana barrier evolution (sensu; Penland 1987; barrier model) when sediment supply is abundant and barrier processes are dominated by spit progradation, storm breaching, inlet development, and aggradation of the flood tidal deltas.

Introduction

Sustaining barrier islands of the Mississippi River Delta Plain (MRDP) is of social, ecological, industrial, and environmental importance. Barrier islands are important coastal landforms that harbor important marine life and help maintain gradients between saline and freshwater systems thereby preserving estuarine systems (Georgiou et al., 2005). Barrier Islands and their sub-environments serve as the primary landform where hurricanes waves dissipate their energy and in many instances lessen storm surge (Georgiou & Schindler, 2009). Currently, barrier islands in Louisiana are in a transgressive phase, undergoing fragmentation and breaching due to ongoing rise in sea level, lack of sediment supply and are subjected to frequent erosion events from storm-induced transport. These processes result in barriers that (1) may be truncated from the seaward side, (2) experience in-place drowning, or is some instances (3) rollover. But, overall barrier island systems in Louisiana experience continued retreat.

The fundamentals of delta and barrier island development and evolution within the MRDP are reasonably well understood (Fisk et al., 1954; Fisk & McFarlan, 1955; Frazier, 1967; Coleman, 1988; Penland et al., 1988). Overall, the MRDP consists of a suite of inter-fingering and overlapping fluvio-deltaic deposits that formed in response to changes in distributary position, sediment supply and basin accommodation space. Within the last 8 ka, the Mississippi River has contributed to the formation of seven delta complexes, constructed of sixteen delta lobes, (Figure 1) (Frazier, 1967) through distributary switching processes. Following abandonment of each delta lobe deposit, individual delta deposits have undergone relative sea level rise and marine reworking, which ultimately contribute towards the formation of deltaic barriers (Figure 2).

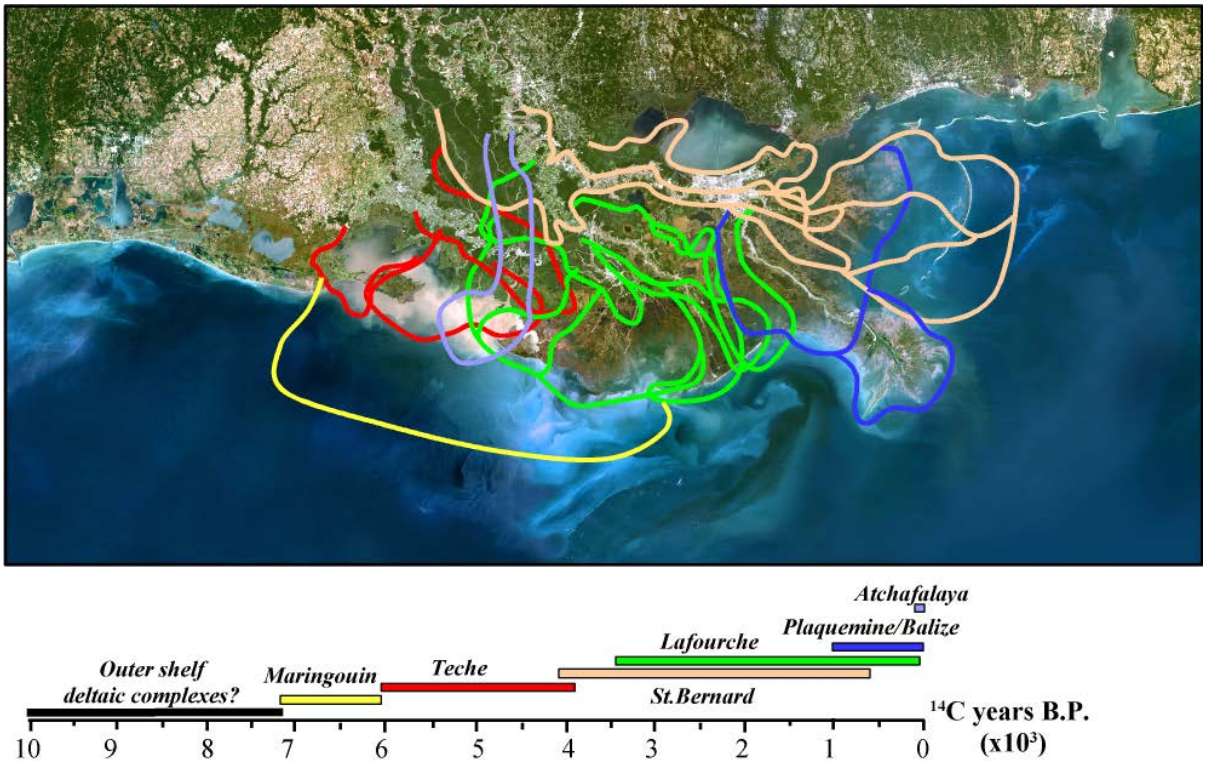

Figure 1: Spatial and chronological delta lobe distribution of the Mississippi River Delta complexes of the last 7–8 ka. Abandoned delta lobes have been reworked by marine processes to form transgressive sandy barrier systems and inner shelf shoals (Kulp et al., 2005).

Figure 2: Model of sandy barrier system development from abandoned deltaic headlands of the Mississippi River Delta Plain (Penland & Boyd, 1988; modified by Blum & Roberts, 2012).

Historical Evolution

The Lafourche complex prograded across parts of the formerly active Teche and St. Bernard Delta complexes (Penland et al., 1987) at approximately 3.5 ka (Frazier, 1967). Bayou Lafourche was the fifth and final active distributary of the Lafourche Delta complex and remained active until approximately 0.15 ka (Penland et al., 1987; Kulp et al., 2005). Progradation of the Bayou Lafourche Delta extended beyond an earlier formed transgressive Teche shoreline, resulting in the interception of longshore sediment transport to form sand-rich beach ridges along the Caminada-Moreau Headland (Ritchie, 1972; Penland et al., 1987; Bird, 2000; Kulp et al., 2005). Subsequently, the Mississippi River diverted flow to the Plaquemines system of distributaries, leading to a reduction of sediment supply to the Caminada-Moreau Headland.

During the last 100 years, the Caminada-Moreau headland has experienced the highest rates of shoreline erosion along the Louisiana Gulf Coast and has retreated more than 3 km (Morgan & Larimore, 1957; McBride & Byrnes, 1997; Miner et al., 2009). Contributing toward this transgression was a 1904 dam construction at Donaldsonville, which deprived Bayou Lafourche of fluvial input and resulted in salt water intrusion 38 miles upstream to the Intracoastal Canal (Dantin et al., 1978). As a Stage 1 barrier system (sensu Penland et al., 1988) that is starved of fluvial sediment input and subjected to impacts from relative sea level rise, marine reworking and transgression, and bidirectional longshore sediment transport of the deltaic headland resulted in the formation of flanking barriers spits, sourced primarily by the Caminada-Moreau headland. These barrier spits were elongated through continued transport of sediment from the headland, often breached to form flanking barrier islands and ultimately enclosing interdistributary bays to the east and west (e.g., Barataria Bay and Terrebonne Bay). During the past 125 years, Timbalier and East Timbalier Islands have migrated (Miner et al., 2009) respectively landward and westward, and landward (~3,000 m; 9,840 ft) into Timbalier Bay (Lombardo, 1992; NOAA, 1998). East Timbalier Island has the highest rate of sub-aerial land loss among all Louisiana barrier islands since 1980 (McBride & Brynes, 1997; Penland et al., 2003, Miner et al., 2009).

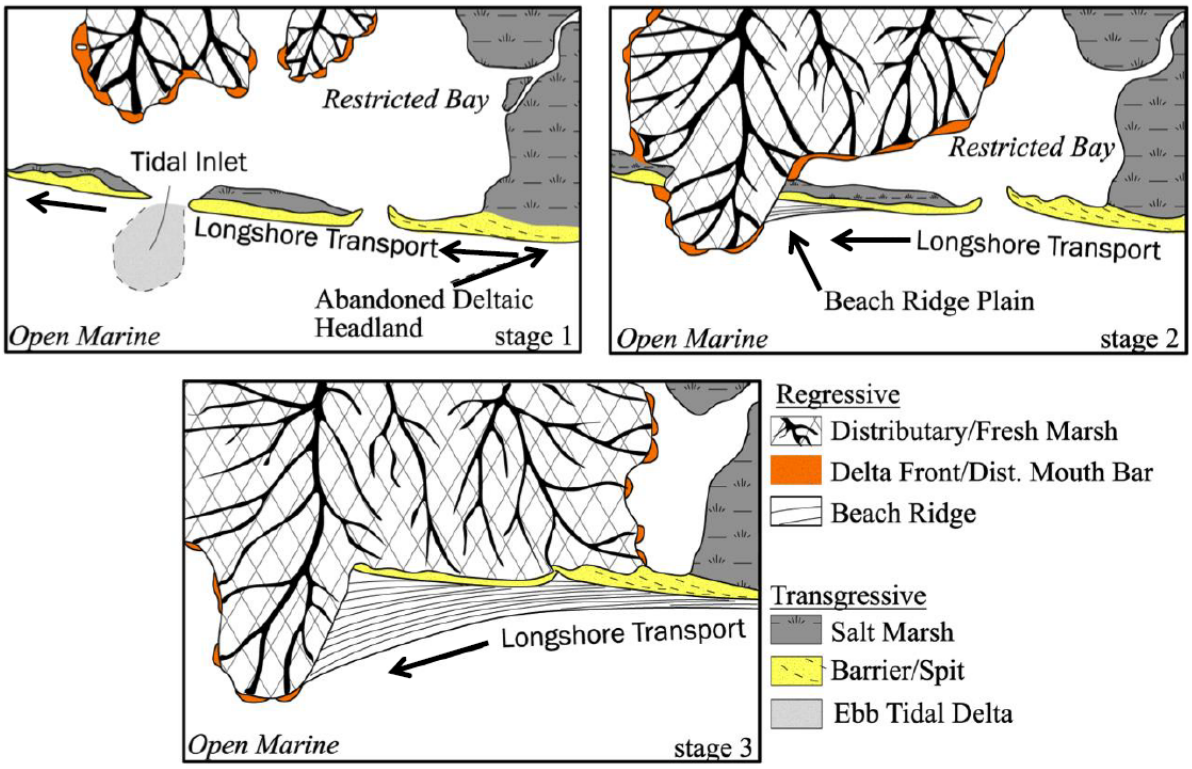

Figure 3: Conceptual model showing the creation of a beach ridge strand plain by erosion of an abandoned headland up-drift of an actively prograding headland (Kulp et al., 2005).

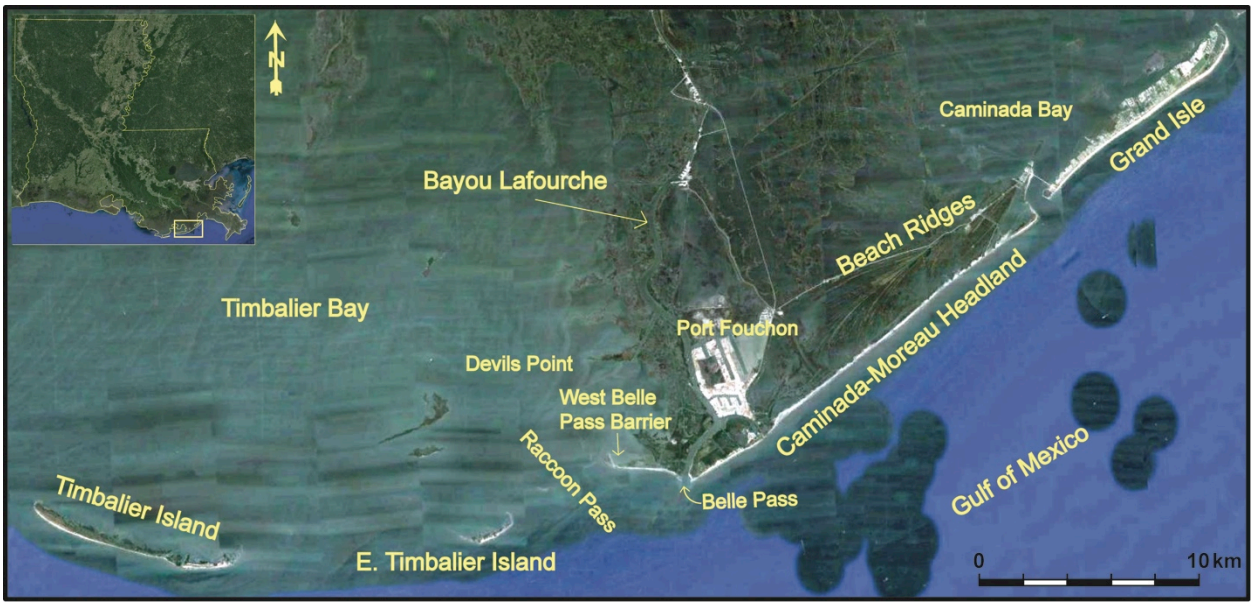

Figure 4: Regional map of the Lafourche Delta barrier system (Aero-metrics image, 2012).

ANTHROPOGENIC ALTERATIONS

The Bayou Lafourche barrier system has undergone geomorphic changes during the last century as a result of high erosion rates, subsidence, frequent storm events, sediment deficit, and anthropogenic modifications. After Bayou Lafourche was dammed in 1904, several coastal modifications were completed in the area for navigational, erosional, and industrial purposes and have altered the geomorphology and depositional patterns in the area. In 1935, parallel 152 m (500 ft) long by 61 m (200 ft) wide rock jetties were constructed at Belle Pass to accommodate navigation from the Gulf of Mexico through Bayou Lafourche to the Intracoastal Canal. Headland erosion resulted in a seaward 90 m (300 ft) jetty extension in 1945. In the 1950's, Bayou Lafourche was dredged and widened (Dantin et al., 1978), and a groin was installed east of the jetties (Figure 4; Mossa et al., 1985). Finally in the 1960's, Belle Pass was relocated by adding a new west jetty and widened to maintain a 97 m (320 ft) wide clearance at Bayou Lafourche. The old west jetty was removed, and both jetties were extended 300 m (980 ft) seaward by 1969 (Figure 3; Figure 4; Mossa et al., 1985). The placement of the jetties and groin at Belle Pass obstructs the westward-directed longshore current as well as transport along beaches on the down-drift side of the headland and limits sediment supply to East Timbalier Island (Mossa et al., 1985; Curole et al., 2012).

Figure 5: Oblique aerial view of the Belle Pass jetties and groin taken after Hurricane Cindy (Cat. 1) landfall on the Caminada-Moreau Headland on July 11, 2005. (Image credit D. Weathers).

Port Fourchon is a major oil and gas depocenter for the Gulf region. An extensive series of access and pipeline canals, more than 62 km (39 miles), have been dredged in Timbalier Bay to support oil and gas production (Penland & Suter, 1988). East Timbalier Island developed into a prominent site for offshore production of oil and gas (Curole et al., 2012) containing approximately 400 oil and gas wells on the island and Timbalier Bay (Miller, 1994). The first attempt to stabilize the island and protect oil and gas infrastructure was in the 1950's when Gulf Oil constructed a (between 2.4 m and 6 m) dirt levee on the crest (several hundred feet landward of the shoreline) of East Timbalier Island. In 1965, three groins were installed, one on the western side and two in the central part of the island, to repair several breaches that occurred during Hurricane Betsy (NOAA, 1998). Later in 1966, the groins were extended 90 km (300 ft), and an additional groin was added west of the central groins. A rock seawall was erected alongshore parallel to the shoreline connecting the groins. By 1974, East Timbalier was encased by a 16 km (10 miles) rock seawall revetment with 30 m (100 ft) groins spaced every 60 m (200 ft) across the island (NOAA, 1998), disrupting sediment supply to the island. Also, the original dirt levee was reinforced with stone to protect the bayside of the island from northwesterly driven waves (NOAA, 1998). The rock seawall revetment and reinforced rock levee were rebuilt in 1974 after they were displaced during Hurricane Carmen (NOAA, 1998). The placement of the revetment and dikes has not completely protected the island against intense wave energy created during frequent storms. The rock revetment has since been left behind in the surf zone and functions as a breakwater as shoreline transgression of the island continues (Figure . 5; Mossa et al., 1985).

Figure 6: Rocks initially placed on the bayside of East Timbalier currently function as a breakwater off the Gulf-side shoreline. (Curole et al., 2012.)

COASTAL PROTECTION AND RESTORATION PROJECTS

The Coastal Wetlands Planning, Protection and Restoration Act (CWPPRA), was enacted in 1990 to provide cost-effective plans for creating, restoring, protecting, or enhancing coastal wetlands. A number of coastal protection and renourishment projects have been implemented within the study area in compliance with the Louisiana's Comprehensive Master Plan for a Sustainable Coast (Figure 6). Beach nourishment projects place beach-compatible sand in the nearshore to replicate protective characteristics of natural dune and beach structures (Penland & Suter, 1988; Campbell & Benedet, 2004). The West Belle Pass Headland Restoration project TE-23 (Figure 6), completed in 1998, was devised to protect the Timbalier Bay shoreline from wave-induced erosion and to renourish the surrounding interior saline marsh from encroachment of Timbalier Bay. Approximately 184 acres of marsh bounded by Belle Pass to the east, the Gulf to the south, and Timbalier Bay to the west were renourished using 1.5 million cubic yards of material that was dredged from Bayou Lafourche. The shoreline protection and containment phase of the project consisted of the placement of an earthen retention dike, a foreshore rock dike, rock closures, and submerged rock weir along East Timbalier, Bayou Lafourche and west of Belle Pass (Curole & Huval, 2004). At a cost of $6.82 million, the project neglected to replenish the marsh as planned due to a deficit of dredged material pumped into the marsh, and storm induced breaches in the containment dike either during or shortly after construction. In addition, vegetated wetlands were severely damaged by marsh buggies during the construction (Curole & Huval, 2004).

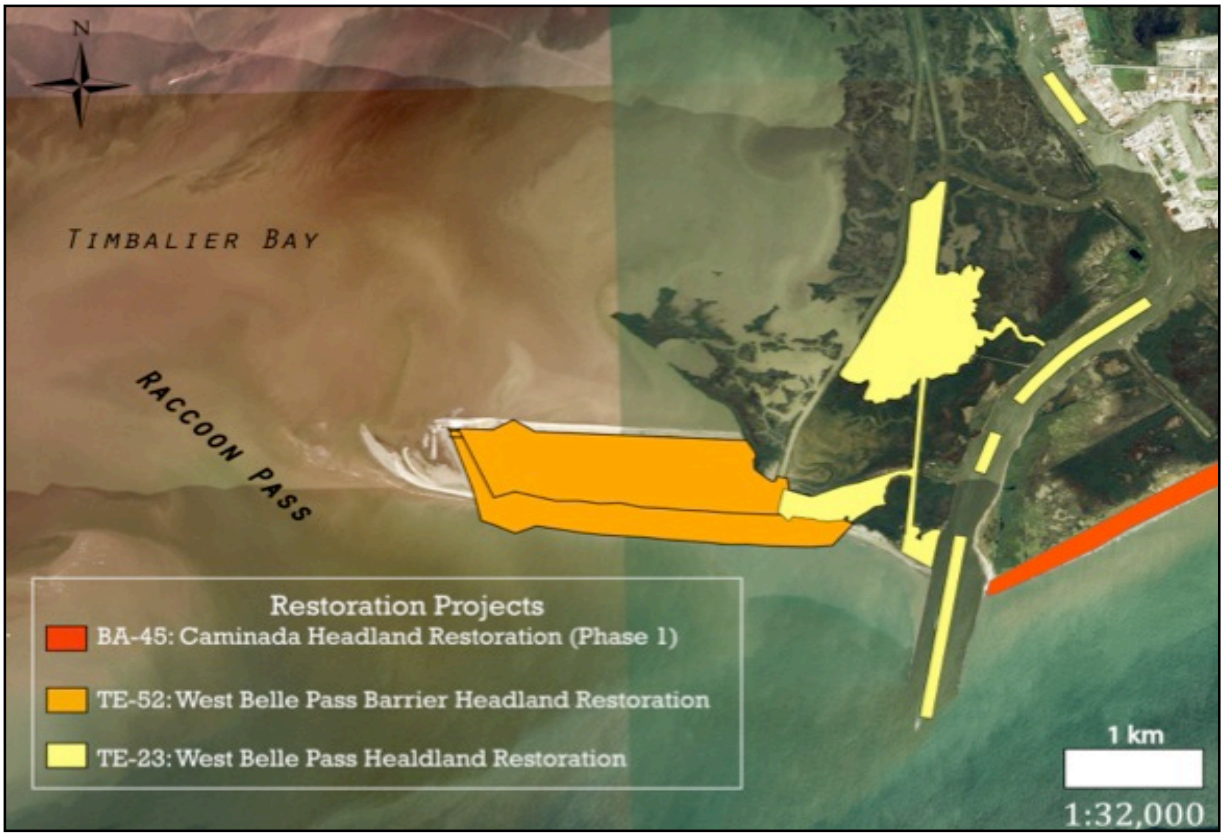

Figure 7: Coastal sediment renourishment projects performed by the Louisiana Coastal Protection and Restoration Authority (CPRA) for the Caminada-Moreau Headland and flanking West Belle Pass barrier system (National Agriculture Imagery Program (NAIP) image; October 2013).

In 2012, the West Belle Pass Barrier Headland Restoration project TE-52 (Figure 6) had been completed at a cost of $42.2 million. This project re-established a large portion of the beach, dune, and back barrier marsh that once existed along the Caminada-Moreau Headland west of Belle Pass. The project area encompassed 411 acres, starts approximately 2,800 ft from Belle Pass and extends west for approximately 8,500 ft (Figure 7). During construction, Hurricane Isaac impacted the project on August 28, 2012. The storm surge recorded in the area reached 5.64 ft MLLW (5.39 ft, NAVD), which resulted in breaches of the containment dike and washover deposition of approximately 104 yds^3 yards of sand (Figure 7). Reinforcement sheetpile was installed where the containment dike breached and sand was replenished (Figure 7; Parker et al., 2012).

The Caminada-Moreau Headland project BA-45, Phase 1(Figure 6), completed in 2014, renourished six miles of beach and dune between Belle Pass and Bayou Moreau through the placement of sediment extracted from Ship Shoal (http://coastal.la.gov/our-work/projects/).

Figure 8: CPRA Restoration Project TE-52 performed on West Belle Pass Barrier, four photos show the containment dike and sediment renourishment progress. A) View from the east of project under construction on August 13, 2012. The west Belle Pass jetty is in the foreground. B) View from the west of project under Construction on August 13, 2012. with a recently formed recurved spit. C) View toward the east on August 31, 2012, after Hurricane Isaac passed directly over the barrier and created a breach in the containment dike and washover deposition of 104 yds^3 of sand. D) View from the west of project on October 1, 2012 after sheetpile closure of the containment dike breach. (Photographs from Weeks Marine & Aerophoto; Parker et al., 2012).

Figure 9: CPRA Restoration Project TE-52 performed on West Belle Pass Barrier, four photos show the containment dike and sediment renourishment progress. A) Arial view from the east of project under construction on August 13, 2012. The west Belle Pass jetty is in the foreground B) Arial view from the west of project under Construction on August 13, 2012. A recurved spit formed from longshore transport processes. C) Arial view from the west of project area on August 31, 2012, after Hurricane Isaac passed directly over the barrier resulted in storm induced breach in containment dike and overwash of 104 yds^3 of sand. D) Aerial view from the west of project October 1, 2012 after sheetpile closure of containment dike breach. Google Earth imagery (center) shows Hurricane track over the project area on August 28, 2012. (Photographs are courtesy of Weeks Marine & Aerophoto for NOAA Fisheries; Parker et al., 2012).

East Timbalier Island was severely breached and inundated by Hurricane Andrew in August 1992. By August 1993, 163 hectares (403 acres) total land area remained (NOAA, 1998). McBride and Byrnes (1997) predicted that East Timbalier Island would disappear by 2097, except for a few fragments remaining. In order to expand life expectancy of the island, the East Timbalier Sediment Restoration project Phase 1, TE-30 and Phase 2, TE-25 (completed in 2001) planned to construct dune, marsh, and shoreline protection features on the heavily deteriorated barrier island (Figure 9). Both projects were performed simultaneously and functioned as a single project designed to create 217 acres of dune and marsh habitats and place rock rubble along breached areas. Although dune and marsh were created, the project was not completed according to the original design due to shoreface changes and inferior

sediment. The shoreline of the island experienced substantial erosion and steepening from planning stage to construction time. The projected earthen and stone containment dike was only completed on the western end of the island leaving a significant amount of the fill areas unconfined. To further complicate the matter, the percentage of sand in the borrow areas was much less than estimated. The use of finer, easily suspended sediment resulted in inadequate dune structures. Dredging was completed January 10, 2000, and out of the 2,065,276 m^3 (2,701,279 yd^3) removed from the borrow site, only 754,884 m^3 (987,351 yd^3) remained in the filled areas after construction (Curole et al., 2012). During the summer of 2002, Hurricane Isidore passed directly over the island and Hurricane Lili to the west and south, reducing the total land area of East Timbalier Island back to near pre-construction level (Curole et al., 2012).

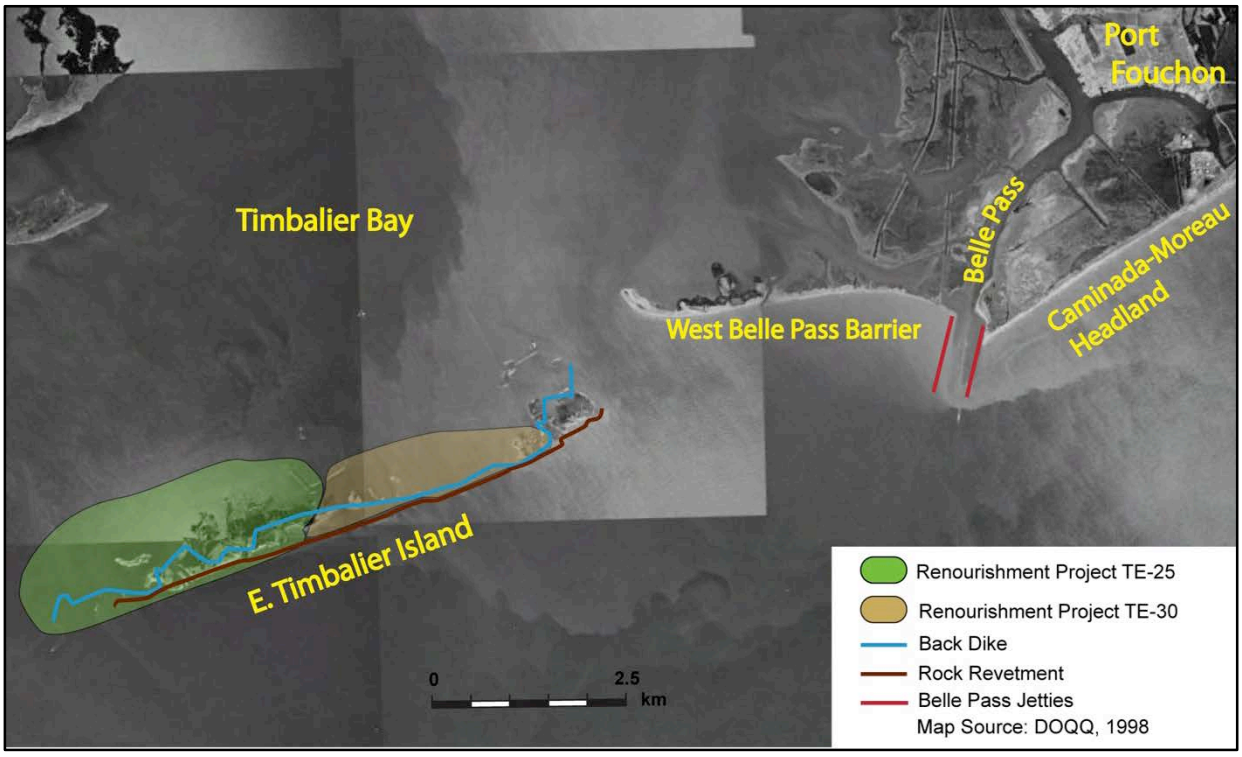

Figure 10: Regional map showing the CPRA TE-25 and TE-30 renourishment projects and locations of rock revetment and dikes on East Timbalier Island (Curole et al., 2012).

Objectives and Deliverables

The main objectives of this study are as follows:

1. To develop a conceptual sedimentary framework and budget of the Bayou Lafourche barrier shoreline located between East Timbalier Island and the Miss Lena - Caminada-Moreau headland, including Raccoon Pass;
2. Identify dominant lithofacies of the barrier system at the surface and in the shallow subsurface;
3. Determine what processes control the distribution of identified lithofacies to provide information about dominant sediment transport patterns that have historically influenced the barrier island system; and
4. Verify dominant transport pattern affecting the current distribution of shallow, barrier platform sedimentary facies.

Data Base and Methods

This study examines the shallow stratigraphic and sedimentological framework and historical evolution of the Bayou Lafourche headland and associated barriers by combining a database spanning 25 years of research archived at the University of New Orleans (UNO) Coastal Research Laboratory (CRL) along with newly acquired vibracore logs and grab-samples (Kramer et al., 2014). The data base combines vibracore and engineering boring logs, grab sample data, high-resolution seismic profiles, bathymetric surveys, historical shoreline data, hydrodynamic data, and satellite imagery to interpret the change in sediment distribution patterns through time and space within the Lafourche Delta region (East Timbalier Barrier Island, Raccoon Pass, and the West Belle Pass region of the Caminada-Moreau Headland). A total of 209 vibracores and 144 grab-samples were used for the study.

VIBRACORES AND GRAB-SAMPLES

Vibracore data for the area between the Caminada-Moreau Headland and Timbalier Island during the period of 1986 through 2003 were selected from database of cores obtained from the Louisiana Geological Survey, CPRA and UNO student research projects. Grab-sample data was obtained from the Louisiana Barrier Island Comprehensive Monitoring (BICM) study (Kulp et al., 2009).

During the summer of 2014, supplemental vibracores and grab-samples were collected throughout the inlet complex on the east side of Timbalier Bay between Raccoon Pass and Devils Point. Locations of six vibracores were selected to fill in gaps in previous data where there were seismic profiles but lacked core data. Some vibracores were correlated to seismic ties, while others were correlated to a single seismic line. Vibracores were obtained on the vessel R/V Greenhead using a Stow G55H gasoline powered vibrating machine. The vibracore machine was coupled with a 20-foot 3-inch diameter aluminum pipe with a 0.050 inch wall thickness. Vibracore pipes were lowered through the water column and vibrated into the subsurface. Measurements were recorded to calculate the degree of compaction associated with the abrupt vibrating motion, which causes the sample to liquefy and settle within the aluminum housing. The aluminum tubing was capped, plugged, and sealed before being hoisted out of the water. The tubes underwent further inspection and capping once brought aboard to ensure an appropriate sample was acquired. Vibracores were then processed at the UNO Pontchartrain Institute's Vibracore Analysis Lab. Each vibracore was cut into halves and visually analyzed to document the sedimentary texture, structure, stratification, and grain size. The cores were digitally photographed and archived. The images are used to create a digital mosaic of the entire core for reference using Adobe Photoshop.

A total of 17 grab-samples were collected using a Petit Ponnar along a transect starting in the northeast corner of Timbalier Bay approximately 2,000 m from Havoline Canal and trends south-southwest towards the flood-tidal delta for approximately 3,800 m into Raccoon Pass. Grab-samples were dried and sieved through ASTM No. 45, 60, 80, 120, 170, and 230 according to ASTM D422 standard procedures to determine grain size distribution. Hydrometer analyses were subsequently performed on samples containing greater than 50 g of silt/clay. Grain size analyses (sand, silt, and clay content) of all core tops approximately 5 cm and all grab-samples were compiled and classified in U.S. Geologic Survey (USGS) SedPlot based on Shepard's classification method. Grain size analyses (percent sand, silt, and clay) of core tops and grab-samples were compiled in an excel spreadsheet and plotted in Esri's ArcMap 10.1 according to sediment classification.

HISTORIC SHORELINE

Shoreline shapefiles of the study area were taken from the suite of BICM shorelines in Martinez et al. (2009) for the 1880's, 1930's, 1996, and 2005. To narrow the gap in time and accurately measure shoreline migration patterns between the 1930's and 1996, maps of the Bayou Lafourche barrier system for the years 1956, 1978, and 1988 were scanned from the USGS Atlas of Shoreline Changes (Williams et al., 1992). Maps were georeferenced to NAD83, using geographic coordinates in and digitized with polylines to represent the parameter of subaerial portions of East Timbalier Island, Caminada-Moreau headland, as well as the back barrier bay shoreline.

STRATIGRAPHIC CROSS-SECTIONS

Three cross-sections using newly acquired as well as archived cores were constructed to establish the stratigraphic architecture of Raccoon Pass and the West Belle Pass Barrier.

LITHOFACIES MAPS

Lithofacies maps of the study area were created in Esri's ArcMap 10.1 for four different time periods 1989, 1998, 2004 and 2014 to represent the evolutionary trends of sedimentation patterns relating to the Lafourche delta barrier system and Raccoon Pass inlet. Lithofacies distribution maps were developed using satellite imagery acquired through USGS's Earth Explorer for 1989 Digital Orthophoto Quarter Quadrangle (DOQQ), 1998 (DOQQ), 2004 (DOQQ) and Aero-metrics for Fall 2012 (DOQQ). Facies for 1989 and 1998 were based on visual interpretation of satellite imagery identifying sedimentary patterns, distinct channels, and geomorphic environments. Vibracores from T-1986 used in cross-sections are more seaward and not used to determine lithofacies during these periods of time. The 1980's historic bathymetric survey map (List et al., 1994; Miner et al., 2009) was overlaid to verify facies interpretation and identify ebb-tidal delta for 1989. Identification of lithofacies for 2004 and 2014 was based on visualization of satellite imagery, sediment classifications of core tops (2004 & 2014) and grab samples (2014) that were available within 1 to 5 years time of interest, bathymetric surveys (List et al., 1994; Miner et al., 2009), historic shoreline data (Martinez et al., 2009) and cross-sections of selected cores (Kulp et al., 2006). Tidal-inlet morphology and sedimentation patterns for each time period were labeled using terminology from Hayes (1979). Stratigraphic cross-sections developed for this study were used to verify interpretations and supplement lithofacies environments where insufficient information was available. Geomorphic features were measured and distances calculated using the ruler tool in ArcMap. Area for geomorphic units was calculated by polygon attributes in ArcMap.

ACOUSTIC DOPPLER CURRENT PROFILERS DEPLOYMENTS

To conduct hydrodynamic observations during winter storms and fair weather conditions, Acoustic Doppler Current Profilers (ADCP) were deployed at the Raccoon Pass and the East Timbalier inlet. The Raccoon Pass inlet deployment measured wave/velocity fields and collected continuous tidal and temperature information at the inlet throat at approximately 3.2 m depth, whereas the East Timbalier inlet deployment measured waves/velocity fields, temperature, and tidal water levels at a depth of approximately 3 m. A *Nortek Aquadopp* Current Profiler was positioned with sensors approximately 0.6 m above the bed at the Raccoon Pass site. The current profiler used 20 cells of 0.25 m depth, starting 0.10 m beyond the transducer. Current profiles were determined using pings averaged for 60 seconds every 30 minutes. The horizontal velocity range detected with this unit is ±10 m/s with an accuracy of 1% of the measured value ±0.5 cm/s. Directional wave data were determined using 2,048 total wave samples with a

sampling frequency of 4.0 Hz every hour. At the East Timbalier inlet a *Teledyne RDI Sentinel V* ADCP was deployed on a trawl resistant tripod and was configured in a similar way as the ADCP at the Raccon Pass site. The deployment period for the Raccoon Pass site was from December 11, 2014 through January 3, 2015 and for the East Timbalier site from December 22, 2014 through January 15, 2015, with an overlap of 11 days. To detect and correlate observations at the inlet with events producing sub-tidal water level variations, continuous data were gathered from nearby meteorological stations operated by the National Oceanic and Atmospheric Administration (NOAA), USGS, and the Coast Wide Reference Monitoring System (CMRS) operated by CPRA. The data included time-dependent wind speed, direction, atmospheric pressure, and tidal elevations with a frequency of 15 minute-to-hourly depending on the station/agency.

DIGITAL FILTERING OF HYDRODYNAMIC OBSERVATIONS

To determine subtidal water variations at the inlets, the team used a sixth order Butterworth filter designed for low-pass filter analysis at a 40-h cutoff period. The Butterworth filter was selected for maximal flatness in the passband response, and near 100 % energy attenuation beyond the transition band. Transfer function coefficients were obtained using the *MATLAB* function 'butter.m'. The transfer function for a sixth order Butterworth filter can be expressed as

$$H(z) = \prod_{k=0}^{2} \frac{b_{0k} + b_{1k}z^{-1} + b_{2k}z^{-2}}{a_{0k} + a_{1k}z^{-1} + a_{2k}z^{-2}} \qquad (1)$$

where

$$b_{0k} = b_{2k} = \Omega_c'^2 ,$$
$$b_{1k} = 2\Omega_c'^2 ,$$
$$a_{0k} = 1 + 2\cos\left[\frac{\pi(2k+1)}{2N}\right]\Omega_c' + \Omega_c'^2 ,$$
$$a_{1k} = 2(\Omega_c'^2 - 1) ,$$
$$a_{2k} = 1 - 2\cos\left[\frac{\pi(2k+1)}{2N}\right]\Omega_c' + \Omega_c'^2 ,$$
$$z = \mathrm{e}^{\mathrm{i}w_c} ,$$
$$w_c = 2\pi f_c \mathrm{T} ,$$

Here, N is the filter order, f_c is the cutoff frequency in hertz, T is the sampling period in seconds, and w_c is the cutoff frequency in π radians per sample. Furthermore,

$$\Omega_c' = \tan\left(\frac{w_c}{2}\right) = \tan(\pi\frac{f_c}{f_s})$$

where f_s is the sampling frequency in Hertz. The product operation returns a function of the form

$$H(z) = \frac{b_0 + b_1z^{-1} + b_2z^{-2} + b_3z^{-3} + b_4z^{-4} + b_5z^{-5} + b_6z^{-6}}{a_0 + a_1z^{-1} + a_2z^{-2} + a_3z^{-3} + a_4z^{-4} + a_5z^{-5} + a_6z^{-6}} \qquad (2)$$

Zero-phase digital filtering was implemented using the *MATLAB* function 'filtfilt.m'. This function uses an extrapolation method to minimize beginning and ending transients, and applies the filter a second time after reversing the signal, resulting in a filter order twice that specified by the transfer function coefficients (i.e. 12th-order).

At a 40-h cutoff period, the transition band is bordered by events shorter than 1 CPD (Cycle per Day) and longer than 0.5 CPD. The tidal signal is thereby extracted while maintaining the signal produced by events 48 hours or longer. Filters of this type were applied to time-series data of wind, current, and pressure.

SUB-TIDAL WATER LEVEL ANALYSIS

To quantify mechanisms contributing to sub-tidal water variations, the team used a simplified approach previously used by Li et al., (2011) which utilized the dominant forms of response to storms and include:

$$\zeta \sim \zeta_{wind} + \zeta_{wave} + \zeta_{pressure} + \zeta_{Coriolis} \quad (3)$$

corresponding to wind-induced setup, wave induced setup, and setup caused by the Coriolis effect as well as the barometric pressure effect. The wind stress effect expresses the balance between the wind stress at the surface and the shear stress of the current at the bed. The approximation can be written as

$$\frac{\partial \zeta}{\partial x} \sim \frac{\tau_s - \tau_b}{\rho g h} \quad (4)$$

where ζ is the surface height as related to mean sea level; ∂x is the distance differential in the direction of the onshore wind; ρ, g, and h are water density (for this study, ρ = 1,020 kg/m^3), gravitational acceleration (9.8 m/s^2), and water depth, respectively. The term τ_s is surface shear stress due to wind and is expressed as:

$$\tau_s = \rho_a C_D W^2 \quad (5)$$

where ρ_a is density of the air (approximated to be 1.2 kg/m^3); W is wind speed; C_D is the fluid-drag coefficient determined by bed type. A drag coefficient of 1.6 × 10^{-3} was chosen corresponding to a silt and sand bed (Masselink, 2003). Similarly, τ_b is written as:

$$\tau_b = \rho C_D V^2. \quad (6)$$

where, ρ is water density and V is depth averaged current velocity. Assuming that the water setup within the bay has a linear slope, it follows from the expression for wind stress that:

$$\zeta_{wind} \sim \frac{\tau_s - \tau_b}{\rho g h} \mathrm{L} \quad (7)$$

where L is the distance across the area of anticipated water setup (in the direction of the wind). The distance across Timbalier Bay, from north to south, is approximately 30 km. Wave-induced setup is estimated by the relation (Guza & Thornton, 1981)

$$\zeta_{wave} \sim 0.17\ \mathrm{Hs} \quad (8)$$

where Hs is the significant wave height. The mean of hourly Hs measurements spanning 12/22 and 12/23 was used for this study.

Barometric pressure is observed to affect water level such that a 1 millibar drop relative to the mean pressure outside of the passing system corresponds approximately to a 0.01 m rise in water level, or more accurately (Dean & Dalrymple 2002),

$$\zeta_{pressure} \sim 1.04 \times 10^{-2} \Delta \mathrm{p} \quad (9)$$

The approximating expression for Coriolis effect-induced setup can be written as:

$$\frac{\partial \zeta}{\partial x} \sim -\frac{fv}{g} \tag{9}$$

which, as with the expression for wind effect, becomes:

$$\zeta_{Coriolis} \sim -\frac{fv}{g}\mathrm{L} \tag{10}$$

Here *v* is the east component of the offshore current velocity (roughly 0.05 m/s considering that the onshore winds are primarily southwestern), and *f* is the local planetary vorticity (Coriolis frequency), a measure of the angular velocity required of a body to maintain equilibrium with the Coriolis force. The Coriolis frequency is determined by the latitude of the site θ (approximately 28.17 ° N) and angular speed of Earth's rotation $\mathbf{\Omega}$ (7.29×10^{-5} Hz): $f = 2\mathbf{\Omega}\sin(\theta)$ using, again, a length (L) of 30 km.

HARMONIC AND TIDAL ASYMMETRY ANALYSIS

Tidal analysis to established harmonic constituents at deployment sites were performed using the software package t-tide (Paulowitz et al., 2002), and tidal asymmetry analysis using methods suggested by Friedrich & Aubrey (1997) and Dronkers (1998) where sufficient information was available.

ROTATION OF WINDS AND CURRENTS

At the Raccoon Pass inlet, current profiler cells were positioned at intervals of 0.25 m from a depth of 0.85 m to 4.6 m. Three beams were implemented to measure the north, east and vertical velocities at a sample period of 20 minutes. The bearing of primary current flow was determined to be approximately N60°W. To observe the components of the current velocity parallel and perpendicular to the inlet's axis, current vectors specified by the northern and eastern components were rotated clockwise 60°, corresponding to a 60° counterclockwise rotation of the coordinate plane. This rotation was calculated by multiplication of the northern and eastern components with the rotation matrix for a negative angle, as shown by.

$$\begin{bmatrix} x' \\ y' \end{bmatrix} = \begin{bmatrix} \cos(\theta) & \sin(\theta) \\ -\sin(\theta) & \cos(\theta) \end{bmatrix} \begin{bmatrix} x \\ y \end{bmatrix} \tag{11}$$

Here, x' and y' are arrays of the transverse and axial components of the current velocity, respectively; x is the eastern component array and y the northern component array. Inasmuch that θ is 60°, leads to:

$$x' = \frac{x + y\sqrt{3}}{2} \text{ and } y' = \frac{y - x\sqrt{3}}{2} \tag{12}$$

A separate deployment (*SentinelV*) was placed within the western adjacent inlet. This inlet was determined to have a similar axis of primary flow – using modern bathymetry collected as part of the East Timbalier Island restoration project (Lee, 2015 – personal communication). Again three beams were implemented for current speed measurements along each axis. Data was recorded in 10-minute bursts beginning at the 40th minute of every other hour, each burst had a sample period of 30.5 seconds. Burst values for depth-averaged current speed and direction were grouped by hour, and each group averaged, resulting in a bi-hourly mean speed and direction. The timestamp for this bihourly approximation was converted to hours as on the basis of the *Aquadopp* Profiler's first measurement (12/10/2014 4:09:42 PM).

Wind velocity data spanning the interval of the profiler measurements was collected from NOAA station 8761724 at Grand Isle, Louisiana, approximately 35 km NE from the profiler deployment, as well as NDBC stations SPLL1 and LOPL1, located approximately 30 km SE and SW of the deployment, respectively.

Hourly mean speed and mean direction values were treated as vectors and reduced trigonometrically to hourly northern and eastern components. The same rotation procedure previously described was performed on this data, allowing for observational comparison of wind and current speed data along the axes of the inlets.

Results

HISTORICAL SHORELINES

Eight shorelines between 1884 and 2005 were digitized and plotted in *ArcMap 10.1*. (1884, 1933, 1956, 1978, 1988, 1996, 2004, and 2005; Figure10).Shorelines were determined using the high-water line on the basis of the wet and dry-beach contact and/or debris line. The BICM program calculated the rate of change for four time periods: historical (1884-2005), long term (1904-2005), short term (1996-2005), and near term (2004-2005). Table 1 provides the results of the time-averaged rate of shoreline change for the respective time periods for the West Belle Pass Barrier (Martinez et al., 2009). These rates are useful for evaluating morphological changes and their possible causes.

Table 1: Time-averaged rates of shoreline change for West Belle Pass Barrier. These rates provided a quantitative analysis of shoreline change for different time periods (from Martinez et al., 2009).

Dates	Average Rate of Change (m/yr)
Historical (1884-2005)	-25.5
Long Term (1933-2005)	-10.9
Short Term (1996-2005)	-17.8
Near Term (2004-2005)	-41.5

On the basis of the magnitude of morphological change and shoreline modification proximal to the West Belle Pass Barrier the entire suite of shoreline datasets has been separated into two epochs. During epoch 1 (1884 – 1956) the barrier system, even with natural and anthropogenic modifications, maintains a much larger subaerial footprint when compared to the area of the island anytime between 1978 and the implementation of major restoration projects. During epoch 2 (1976 – 2005), however, the barrier spit system is dominated by shoreline transgression and several restorative shoreline projects that influenced the morphological response of the barrier.

The following sections highlight some of the fundamental characteristics of the historic shorelines within each of the two designated epochs.

Epoch 1

A. 1884

The 1884 shoreline is the oldest available and is the starting point for an evaluation of the historical geomorphologic evolution (Figure10). In 1884 a tidal inlet, approximately 2-km wide, separated West Belle Pass Barrier and East Timbalier Island and is the earliest indication of Raccoon Pass. Although not completely visible in figure 8, the 1884 map shows three outlets to the Gulf of Mexico stemming from Bayou Lafourche: Belle Pass, Pass Fourchon, and Bayou Moreau. The latter two passes are located just east of the area shown in figure 10.

B. 1933

The 1933 shoreline represents the first available shoreline with which morphological comparisons can be made (Figure10). Both natural and anthropogenic events affected the shoreline evolution between 1884

and 1933. In 1904, Bayou Lafourche was separated from the Mississippi River at Donaldsonville, Louisiana, reducing sediment-laden freshwater input to the coastal barriers. In 1915 an unnamed category 3 hurricane made direct landfall on East Timbalier Island contributing toward a net loss of subaerial land between 1884 and 1933, along with widening of Raccoon Pass and closure of all but one of Bayou Lafourche's passes to the Gulf. The damming in 1904 reduced the flow of water reaching the passes, which lead to the partial closure of Belle Pass and full closure of Pass Fourchon and Bayou Moreau (Dantin et al., 1978). Dantin et al. (1978) showed that the shoreline just east of Belle Pass receded 1,128 m from 1885 to 1932 at an average rate of 24 m/yr. However, Dantin et al. (1978) argue that if the damming of Bayou Lafourche in 1904 represents the true onset of sediment deprivation and significant morphologic change, then the rate of shoreline change is even higher at 41 m/yr (1904-1932).

C. 1956

The 1956 dataset depicts a rather dramatic change in the morphology of East Timbalier Island and West Belle Pass Barrier compared to the 1933 shoreline (Figure10). In 1935 Belle Pass jetty construction began at the mouth of Bayou Lafourche. Two tropical storms impacted the study site approximately 3.7 km to the east of Belle Pass in 1936 and 1939. By 1940, the installation of the jetties at Belle Pass was complete, resulting in jetties 152 m long and 61 m apart at the entrance of Belle Pass (Dantin et al., 2978). Five years later, the jetties were extended 90 m shoreward along with a groin east of the jetty system in 1950 (Mossa et al., 1985). The new jetty extensions were 122 m apart and attached to the older jetty sections through transitional sections (Dantin et al., 1978). Despite the presence of these hard structures, the entire flanking barrier system is nearly continuous at this time with less than 0.4 km of water between East Timbalier Island and West Belle Pass Barrier. Even with the installation and modification of the jetties, both barrier systems had a net increase of subaerial acreage between 1933 and 1956. After the 1956 dataset, the distance between East Timbalier Island and West Belle Pass Barrier only increases.

Epoch 2

D. 1978

Between 1956 and 1978, the West Belle Pass area underwent a tremendous amount of shoreline modification, and 1978 marks the beginning of Epoch 2 morphologic change (Figure10). A total of six significant events occurred between 1958 and 1969. In 1958, Belle Pass at the mouth of Bayou Lafourche was dredged and widened to a bottom width of 30 m and a depth of 3.7 m (Dantin et al., 1978). In 1963, the west jetty was relocated to make the distance between jetties 98 m. In the same year, Bayou Lafourche was widened again, resulting in a channel depth of 38 m wide and 3.7 m deep (Dantin et al., 1978). During this widening, the channel was moved west of the already in-place west jetty. The previous channel contained by the jetties was plugged, and there was essentially no west jetty as the old west jetty acted as the "new" east jetty.

Two major hurricanes impacted the region before 1978. Hurricane Betsy made landfall in 1965 as a category 4 storm less than 9.2 km east of Belle Pass. The second storm, Hurricane Carmen, made landfall in 1974 as a category 4 storm just west of the Isles Dernieres, 101 km west of Belle Pass. Sometime between 1956 and1978, Raccoon Pass became established as the main tidal inlet separating East Timbalier from the Caminada-Moreau Headland. The shoreline no longer continued to translate landward

in a continuous, linear fashion as indicated by previous shorelines. Rather, signs of a slight clockwise rotation begin to emerge on west side of West Belle Pass Barrier.

E. 1988

Prior to the 1988 shoreline, the only notable anthropogenic modification that occurs in the study area was on East Timbalier Island, where T-groins were installed on the island to limit the movement of sediment (Mossa et al., 1985) and to limit the magnitude of island thinning that was taking place prior to 1978. Despite these mitigation efforts, East Timbalier continued to thin at its center prior to 1988, and continued shoreline rotation took place along with net widening of Raccoon Pass leading up to 1988.

F. 1996

Between 1996 and 2005, only gulf-side shoreline data is available and estimates of subaerial barrier acreage cannot be accurately determined on the basis of the shoreline data.

By 1996, the clockwise rotation documented by previous datasets is masked by a well-pronounced spit, suggesting that sediment supply was adequate enough for westward progradation into Raccoon Pass (Figure10). Furthermore, a section of East Timbalier Island detached from the main island and was situated between East Timbalier and Raccoon Pass, and herein is referred to as remnant East Timbalier. Interestingly, the orientation of East Timbalier proper and the separated section compared to West Belle Pass Barrier were not the same. Both sections of East Timbalier Island had a shoreline strike of northeast to southwest, whereas West Belle Pass Barrier had a shoreline strike of east to west.

G. 2004

The 2004 shoreline was imprinted by three events, which had the potential to alter the barrier morphology (Figure 10). Captured in the 2004 image is an indication that the West Belle Pass Barrier was transgressing landward and concomitantly eastward through a process of clockwise translation. In 2004 the length of the West Belle Pass Barrier shoreline was approximately half of the 1996 length, and Raccoon Pass widened since 1996.

Two coastal mitigation projects were completed within the study area between 1998 and 2000. TE-23 and TE-25 projects resulted in an array of coastal modifications, including marsh creation, shoreline protection structures, and channel dredging. The outlines of these projects are shown on Figure 14. Additionally, Tropical Storm Isidore, in 2002, made direct landfall through the study site and impacted the shoreline protection efforts of 1998 and 2000.

H. 2005

By 2005, East Timbalier proper and West Belle Pass Barrier were separated by approximately 6.4 km. The 2005 shoreline shows signs of significant erosion and the addition of sediment to maintain a subaerial status, particularly for the remnant island of East Timbalier and West Belle Pass Barrier (Figure 10). Two major storm impacts to the area occurred prior to the 2005 morphology. Hurricanes Cindy (category 1) and Hurricane Katrina (category 3) made landfall approximately 18 and 74 km east of Belle Pass, respectively. The result of these impacts and preceding shoreline morphology prompted legislators to approve the TE-52 project in 2006.

Recent Imagery

Eight images corresponding to eight timeframes were acquired from USGS Earth Explorer to document morphologic change on the west side of the Caminada-Moreau Headland, with a primary focus on the West Belle Pass Barrier and the eastern portion of East Timbalier Island within the last 30 years (Figs. 11&12).

A. November 1989

The 1989 image shows West Belle Pass Barrier separated from East Timbalier Island by a well-developed Raccoon Pass and flood-tidal delta. The West Belle Pass Barrier was approximately 3.1 km long from the end of the recurved spits, where it was cut by an overwash channel, to the west jetty rocks at Belle Pass. There appeared to be one main tidal channel with two smaller channels branching away. Three or four recurved spits were present on the west end of West Belle Pass Barrier. All of these spits were cut by overwash channels. Spits on both sides of Raccoon Pass indicated the dominant sediment transportation pathways, as well as the formation of the flood tidal delta located within Timbalier Bay. This is the earliest image in which hard structures such as rock revetments were visible on the gulf side of East Timbalier Island. Furthermore, it is the only image that clearly showed the extent of the tidal channels associated with Raccoon Pass.

B. February 1998

In 1998, a 1.3 km-long section of East Timbalier separated from the main island (Figure 16), which remained in the same location until it was completely submerged in 2013. This was the first image in which separation is visible between the gulf-side rocks and remnant East Timbalier. West Belle Pass Barrier thinned and elongated towards the west, forming a well-developed spit. At that time, it was approximately 4.5 km from the end of the spit to the west jetty rocks at Belle Pass. Approximately 1.6 km east of the spit, the West Belle Pass Barrier was breached, allowing for the temporary transport of sediment from the shoreface to the backbarrier. Raccoon Pass trended approximately northwest to southeast with a slight bend towards the north in the most northern reaches of the inlet. The various tidal channels were not as visible as in the 1989 image; however, the main channel was noticeable enough to infer the direction of sediment transport through the inlet. Erosion of the West Belle Pass Barrier prompted the acceptance of the TE-23 restoration project in 1992, which was completed in 1998.

C. January 2004

A 2004 image shows drastic changes to the morphology of West Belle Pass Barrier, as well as the location and orientation of Raccoon Pass. In 2004, the subaerial portion of West Belle Pass Barrier decreased in size relative to the 1998 image. In 2004, West Belle Pass Barrier was only 2.4 km long from the west end of the mainland to the west jetty rocks at Belle Pass. However, extensive washover platforms along with numerous breaches were present. By 2004, the thalweg of Raccoon Pass trended approximately west with a slight northeast meander on the bayside.

These changes were most likely the result of three tropical cyclones between 2002 and 2003; one of which, Isidore, was a direct hit to East Timbalier Island. Hurricane Isidore reached maximum strength off the Yucatan Peninsula as a category 3 hurricane. As it continued to move north, it was downgraded to a tropical storm that made landfall within 1.6 km of Raccoon Pass. Isidore made landfall as a tropical storm on September 26, 2002 with sustained winds of 56 knots (Roth, 2010). Tropical storms Bertha and Bill

made landfall within 83 km of Raccoon Pass in August 2002 and June 2003, respectively, and would have contributed to the 2004 morphology.

D. October 2005

The subaerial extent of the barrier system in 2005 is similar to 2004, especially toward the most eastern section of West Belle Pass Barrier. The West Belle Pass Barrier was 2.3 km long and contained numerous breaches. The west side of the image captured subaqueous dunes that are not evident in any earlier images. The dunes were oriented along a northwest trend, approximately 152 m long and 183 m wide. In 2005, Raccoon Pass maintained an east to west orientation, suggesting that processes at work in the 2004 image continued to act on the tidal inlet in 2005. Sections of the rocks at remnant East Timbalier Island were either submerged or relocated from their original position. In the summer 2005, Hurricane Cindy with sustained winds of 65 knots (Stewart, 2006) made landfall as a category 1 hurricane approximately 19 km east of Raccoon Pass, and Hurricane Katrina made landfall less than 74 km east of Raccoon Pass with north winds of 110 knots (Roth, 2010).

E. August 2009

By 2007, the erosional effects of hurricanes Cindy and Katrina had been partially annealed with infilling of all the earlier formed breaches and a continuous 2.7 km of the West Belle Pass Barrier shoreline. In 2008, Hurricane Gustav made landfall as a category 2 hurricane less than 28 km west of Raccoon Pass with gusts of 75 knots in the vicinity of Raccoon Pass (Beven II & Kimberlain, 2009). An examination of the 2009 image reveals two sand deposits with an array of recurved spits that were not present in the 2007 image, mostly along the western terminus of the West Belle Pass Barrier. By 2009, West Belle Pass Barrier had an extended spit, relative to earlier periods, and a shoreline length of 3.2 km measured from spit end to the west jetty rocks at Belle Pass. Remnant East Timbalier and West Belle Pass Barrier proper were separated by 3.4 km of water. The rocks at remnant East Timbalier are completely submerged or destroyed by this time, as they are not visible on the image. Additionally, oil and gas infrastructure originally located on the backside of East Timbalier had now been removed from the shoreface of what remains of remnant East Timbalier Island.

F. August 2010

The 2010 morphology closely resembled that of the 2009 morphology, except for a few subtle differences. For example, a portion of the spit near the west end of the West Belle Pass Barrier in 2009 appeared to be just under the water surface in 2010. There seemed to be more dispersed sand on the west side of West Belle Pass Barrier that was exposed during low tide. Also, remnant East Timbalier had a *V*-shaped morphology with more sand deposition on the west side predominantly within the intertidal to subtidal zone. The channel of Raccoon Pass was poorly imaged in 2010, and consequently no conclusions can be drawn about the pass morphology.

G. October 2012

In 2012, the morphology of the West Belle Pass Barrier was completely altered due to the TE-52 project. At that time, the West Belle Pass Barrier had approximately 3.4 km of shoreline and was 0.6 km wide. A containment dike was located on the bay side and a breakwater located on the southwest corner of the barrier. Conversely, remnant East Timbalier Island had undergone substantial erosion since 1989 and had minimal subaerial area.

In 2012 Hurricane Isaac made landfall as a category 1 system approximately 19 km east of Raccoon Pass, causing damage to Grand Isle and surrounding wetlands with minimal impact to the TE-52 project

H. October 2013 N

The final image of the series shows a system that most closely resembles the modern configuration. The 2013 image shows the effects of natural processes, such as waves, acting on placed sediment to create a 1.3 km-long spit on the west side of the West Belle Pass Barrier. In 2013, the barrier had a shoreline length of approximately 4.3 km and a width of 0.6 km. Although no major storms impacted the area since Hurricane Isaac in 2012, remnant East Timbalier Island was reduced to a subaqueous shoal. Lastly, Raccoon Pass's orientation resembled that of the previous inlet orientations before the 2004-2005 hurricane season.

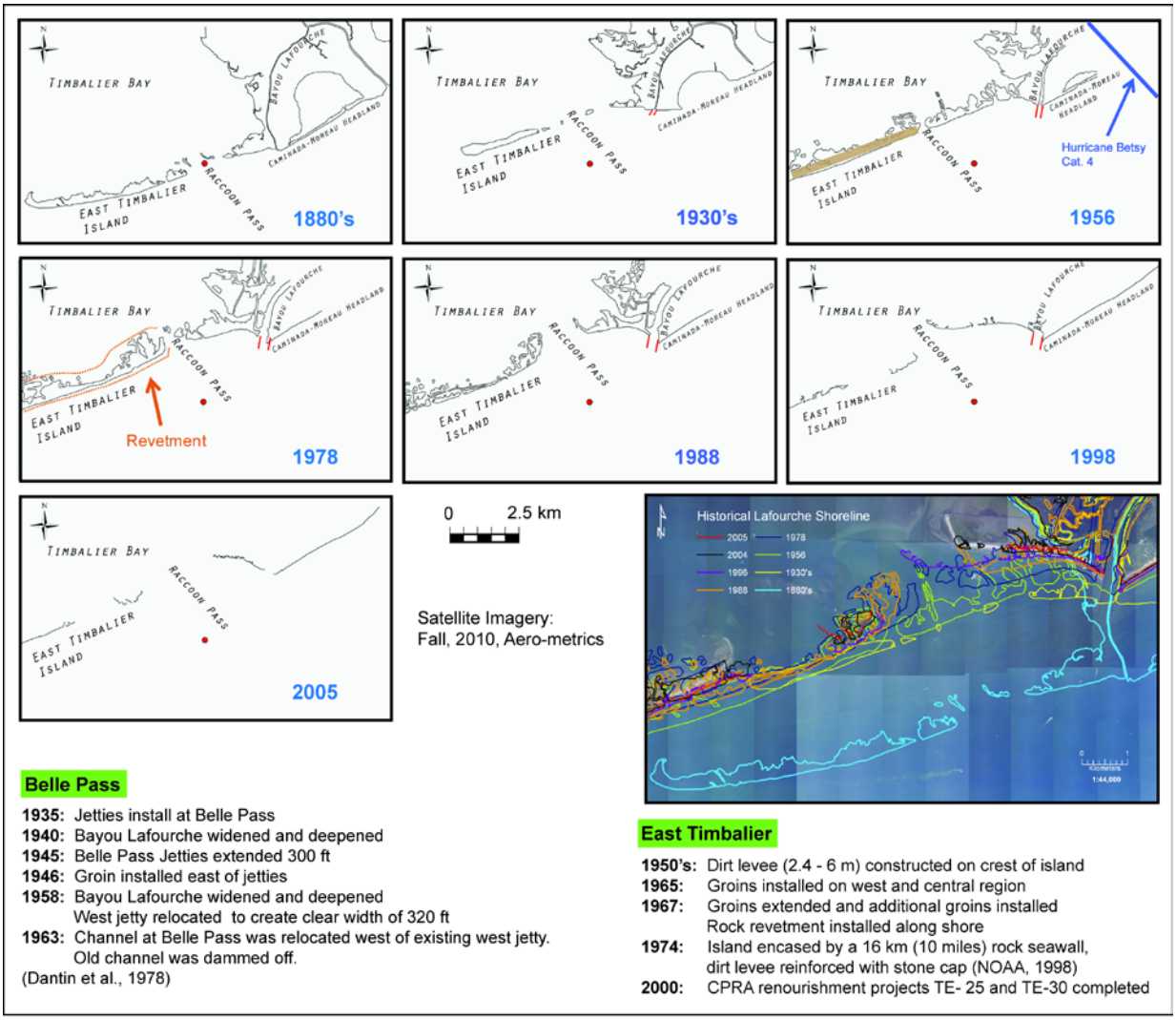

Figure 11: Historic trends of the shoreline geomorphology and a list of the anthropogenic modifications that contributed to the changes in the shoreline.

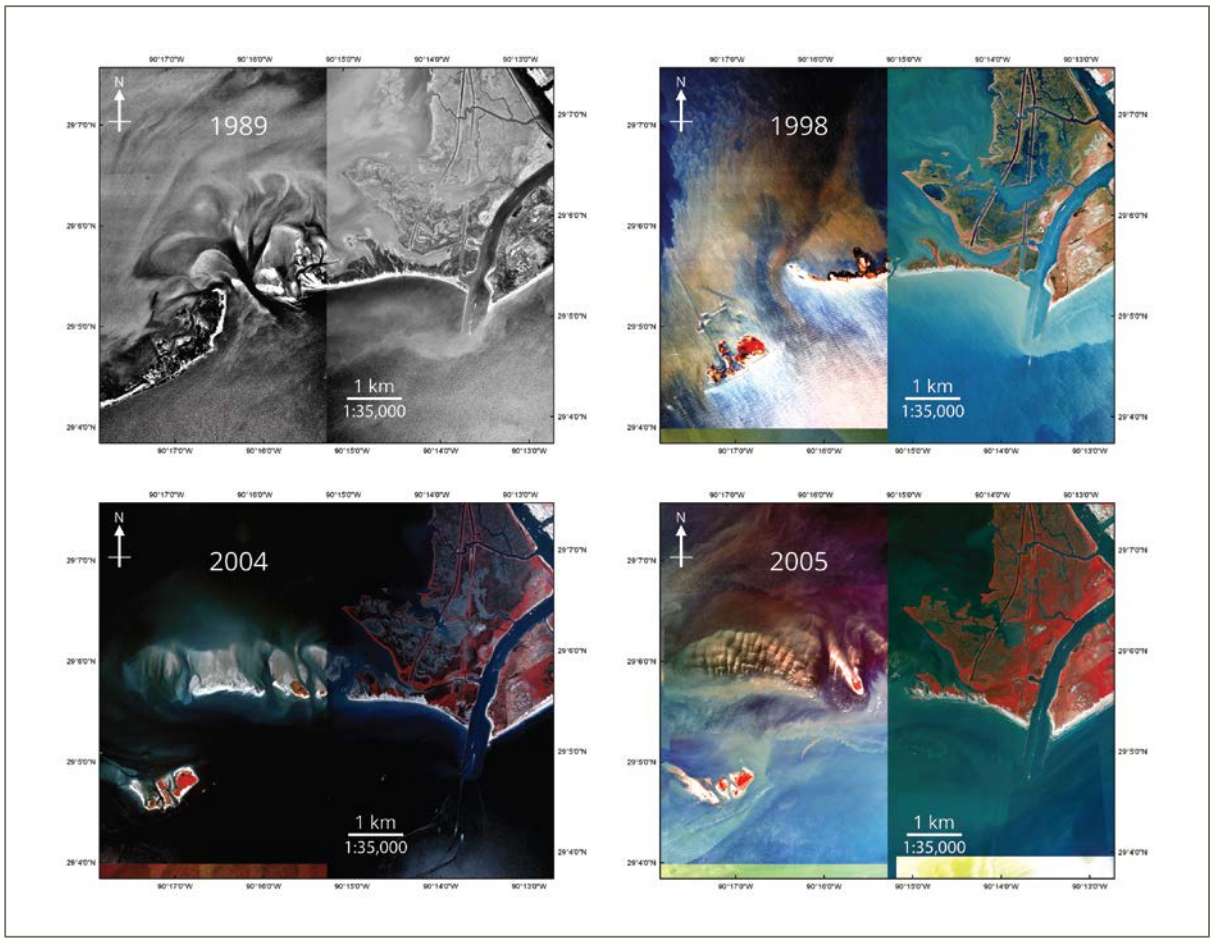

Figure 12: Four digital orthoquads that captured the morphological changes undergone by the West Belle Pass Barrier and parts of East Timbalier Island between November 1989 and October 2005 (USGS Earth Explorer).

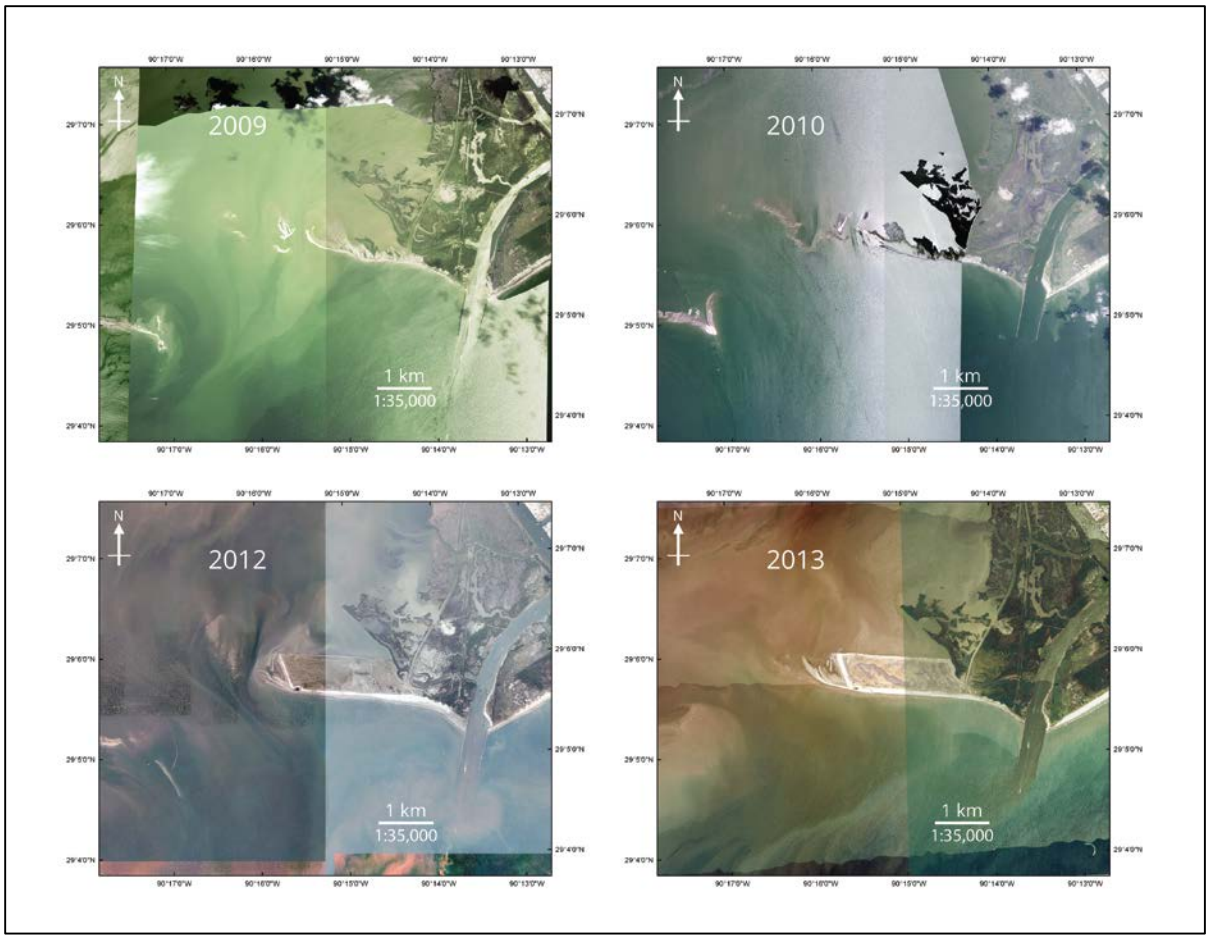

Figure 13: Satellite images showing the morphological changes of the West Belle Pass and parts of East Timbalier Island, between August 2009 and October 2013 (NAIP imagery and orthorectified imagery from USGS Earth Explorer).

Modern Facies Classification

To classify surficial sediments of the identified geomorphic units, grab samples and vibracore tops (upper 2.5–5 cm) were classified using the Shepard (1954) grain-size scheme. The sand content of each of the samples was then plotted (Figure13). Once grain size was determined, each sample was placed within a geomorphic unit/depositional environment. Using the grain size data coupled with satellite imagery, a modern (2014) surficial facies map was created to better understand the likely distribution of these facies (Figure 14). Temporal resolution, however, is poor considering that the first and last samples collected span approximately13 years. It is worth noting that the majority of cores not acquired in 2014 were sampled between 2001 and2003. The author assumes that most of the back barrier sand percentages would not change significantly from 2001 to 2014; however, samples located near the fringe of the flood-tidal delta may experience an increase in sand. Nonetheless, sediment samples coupled with satellite imagery allowed for the classification of surficial sediments in and around Raccoon Pass.

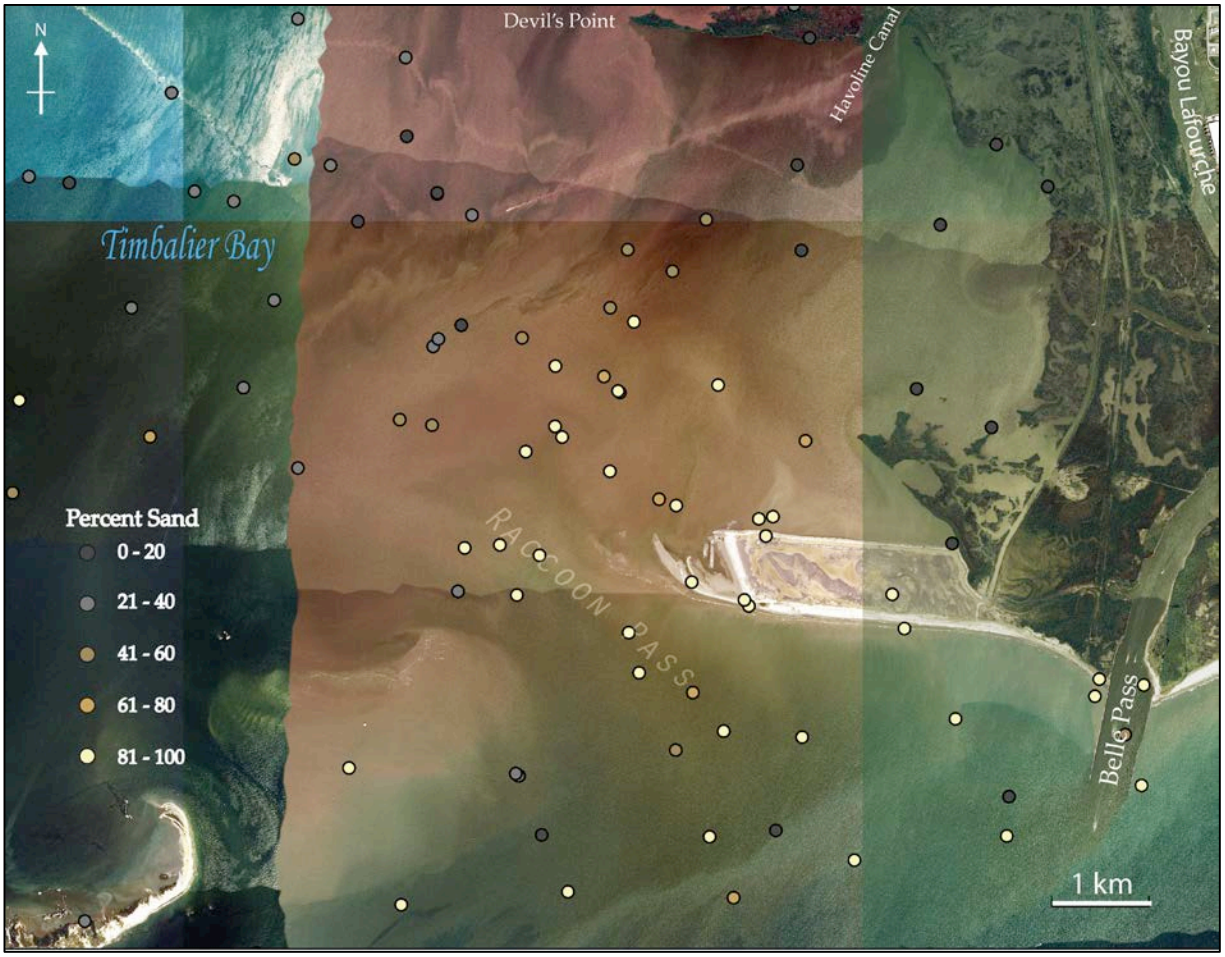

Figure 14: Map of grab and core samples used in this study to construct a surficial facies map. Color ranges show the percent sand of each sample using the Shepard (1954) scheme. (2013 base map).

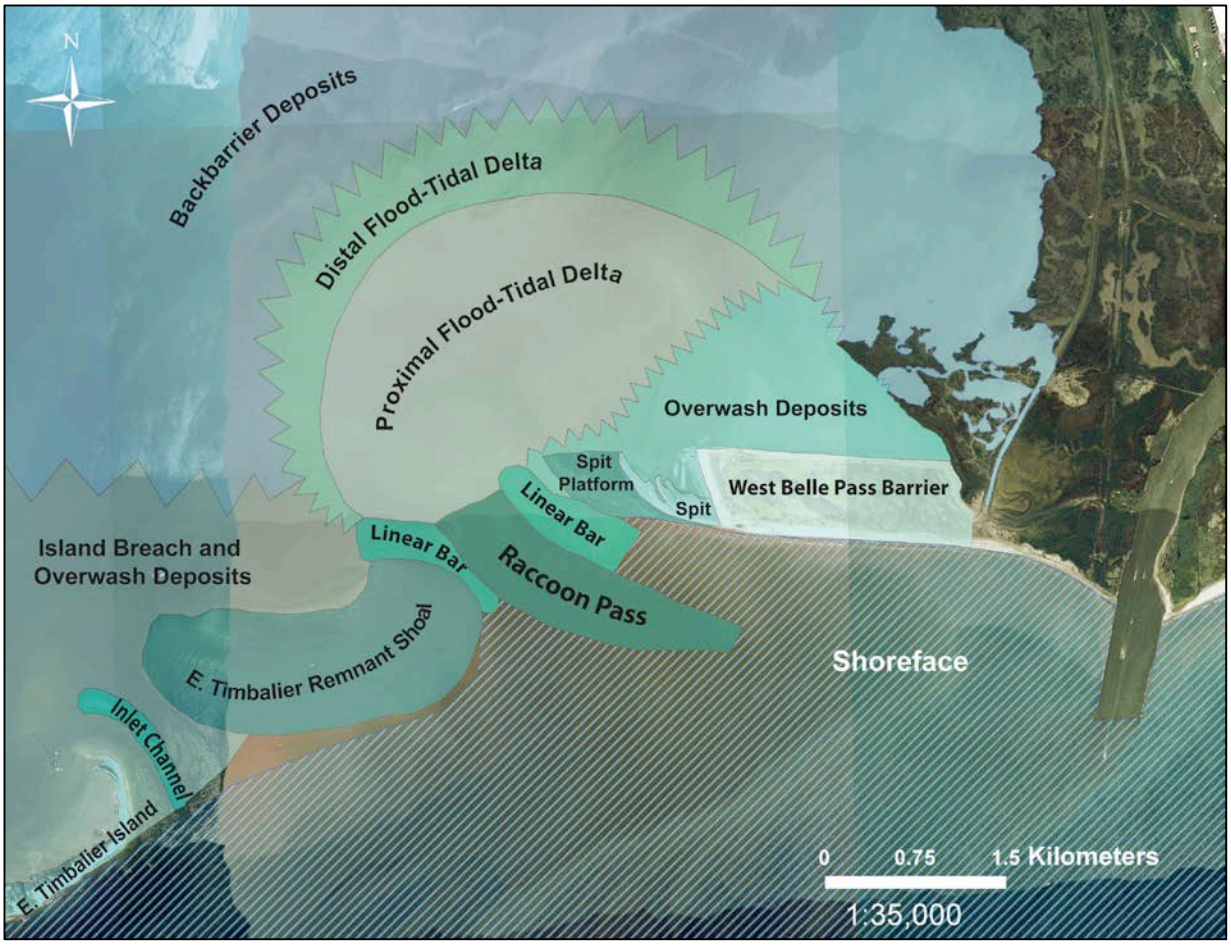

Figure 15: Map showing the distribution of depositional environments on the basis of sand content and imagery.

SUBSURFACE INTERPRETATION

A total of 15 vibracores were used to construct a depositional-dip and a shoreline parallel stratigraphic cross section to show the stratigraphic variability of the study area (Figs. 15 and 16). The deepest core of these cross sections penetrated 5.5 m into the subsurface and the shallowest was 2.25 m. On the basis of the vibracore descriptions, grain size analysis, and imagery, six primary facies were established: 1) Barrier facies, 2) Flood-tidal delta facies, 3) Washover facies, 4) Backbarrier facies, 5) Deltaic facies, and 6) Marsh facies. Due to their backbarrier proximity to one another, relative similar timing of deposition, and textures, flood-tidal delta and washover sands were difficult to separate; therefore, they were treated as one backbarrier facies. Only one core (LH-03-06) contained likely marsh deposits. It was dominated by olive gray, organic-rich clay and will not be discussed further because it is not a significant portion of the stratigraphy. Three main facies are discussed in detail due to their significance and spatial extent: backbarrier facies, flood-tidal delta facies/washover facies, and deltaic facies.

A. Backbarrier Facies

This unit is generally 1-2 m thick, except in cores RP-14-07 and SCC01_56 where it is approximately 2.75 m thick and absent, respectively. This facies unit is dominated by light-gray clay to medium dark-gray clay and light gray to medium gray silty to sandy clay with rare 0.1–0.5 m thick sand layers. This

interval is highly bioturbated and contains fragmented shells less than 5 mm in length with few whole shells of *Rangia*. Dark organic detritus were present throughout much of this facies. Backbarrier facies overlie deeper, regressive deltaic facies and are subjacent to flood-tidal delta and washover deposits, except where it reaches the seafloor. It has a generally gradational bottom contact with the deltaic facies and a sharp, erosional contact with flood-tidal delta and washover deposits.

B. Flood-tidal Delta and Washover Facies

One predominantly sandy package exists stratigraphically above the backbarrier facies. This unit generally contains more than 50% sand and, in some cases, has as much as 90-95% sand (e.g., core RP-14-07). The unit consists of mostly fine dark-gray to light-olive gray sand and is in sharp contact with the underlying unit, indicated by a noticeable increase in sand and silt relative to the clay-dominated backbarrier facies. Due to the morphological changes documented by the historical shorelines, it is evident that sand deposited from overwash processes and sand deposited through the inlet overlap and interfinger. However, the two can be distinguished on the basis of texture and color. Washover facies are generally lighter in color, ranging from light yellowish gray to moderate yellow and consist of approximately 90-95% sand, whereas flood-tidal delta sand percentages are 30-90%. Specifically, washover facies are most likely to be found in cores RP-14-07 and RP-14-09 as opposed to SCC01_56.

Flood-tidal delta deposits can be separated in to proximal or distal deposits on the basis of sand, silt, and clay percentages. Proximal deposits contain more sand and fragmented *Mulina* shells due to the higher energy environments near the tidal inlet. Distal flood-tidal deposits are located along the fringe of the proximal flood-tidal delta and have contained a larger percentage of silt and or clay.

C. Deltaic Facies

The deepest unit encountered in the vibracores consists of very fine to fine-grained beds and lamina containing dark to medium gray and tan to reddish brown fat clay with collective thicknesses that range from a few cm to several m; locally, lenticular fine-grained sand is interbedded within the unit. Whole and disarticulated shell are virtually non-existent within this unit. Kulp et al. (2003) noticed that the sand-rich intervals of this unit vertically correlate updip with the trend of a distributary network located a few km northwest of the study site. On the basis of stratigraphic location and the sedimentary characteristics, this unit is interpreted to have been deposited within delta front and prodelta environments associated with a previous distributary of the Bayou Lafourche distributary system. Discrete sand packages between 0.1-1.0 m that are in sharp contact with fat clay are interpreted to be a part of the distributary channel network. Overall, clay content increases dramatically on the Gulf side of the West Belle Pass Barrier, indicating a lack of sandy environments or shoreface erosion during transgression.

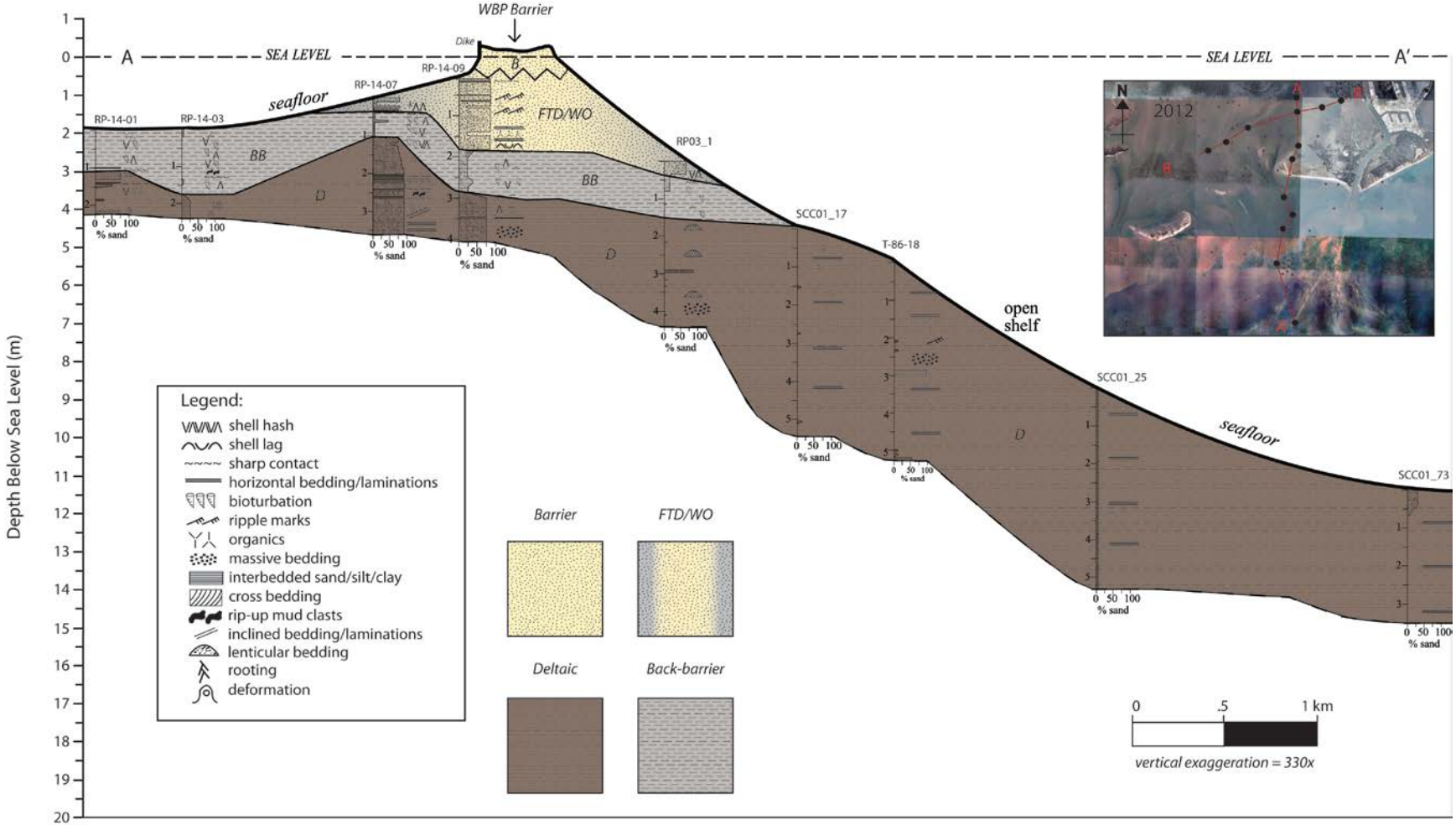

Figure 16: Stratigraphic line of section that shows the stratigraphic variability from Timbalier Bay to the north to the Gulf of Mexico. The inset shows the location of the cross sections with respect to the 2012 shoreline morphology.

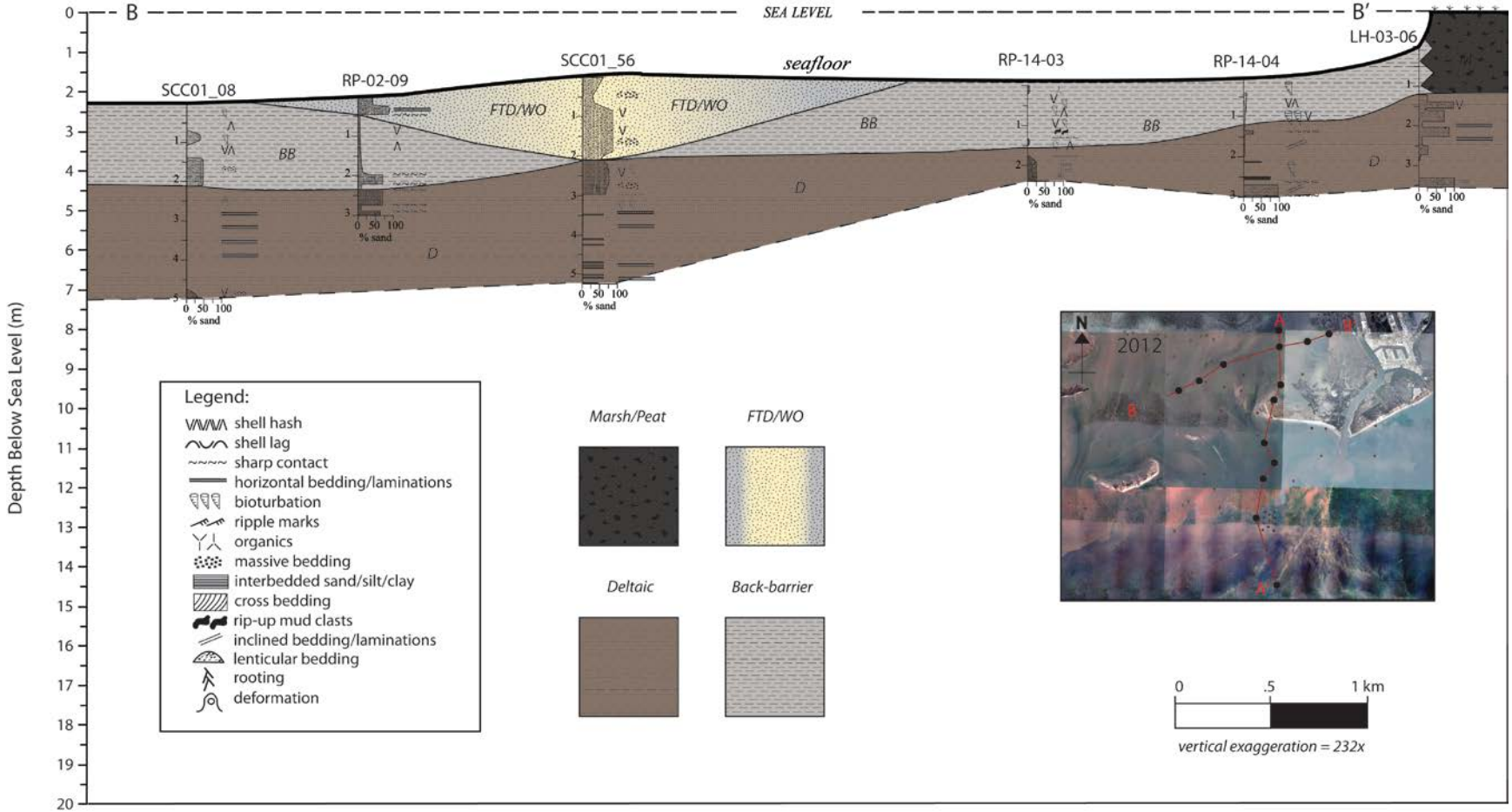

Figure 17: Stratigraphic cross section that shows the stratigraphic variability from west to east within the backbarrier environment of Timbalier Bay. This section shows the thick, primarily clay, backbarrier strata tested during the consolidation section of this study. The inset shows the location of the cross sections with respect to the 2012 shoreline.

Meteorology

For the instrument deployment period between December 2014 and January 2015, wind data was downloaded to determine trends, through wind rose analysis, of the wind direction and magnitude. These data were necessary to establish correlations between meteorological events and local hydrodynamic conditions at the inlets. Figure 17 shows that while the wind rose analysis for the entire year shows wind distribution for various directions of the azimuth, the smaller events are dominate from the northwest quadrant in terms of frequency, whereas the larger events have a more southerly component. During the deployment period, the dominant wind events had a southwesterly component, with gusty conditions that exceeded 12-14 m/s in magnitude. These conditions can often create setup within the backbarrier bay, as evident by the tidal variation, where there is a strong sub-tidal signal (Figure 17, bottom, heavy solid line). The event of the third week of December (18^{th}-23^{rd}) caused sub-tidal variations and a setup due to pressure and wind-induced forcing of the order of 20 cm, which is nearly 35% of the tidal range the system experienced that day (Figure18). Immediately after the storm passed, pressure and wind direction changed appreciably, imposing a rapid set down of the system of 30 cm (more than the setup). Post storm, the slow recovery of the barometric pressure is evident in the depressed tidal range immediately following the storm.

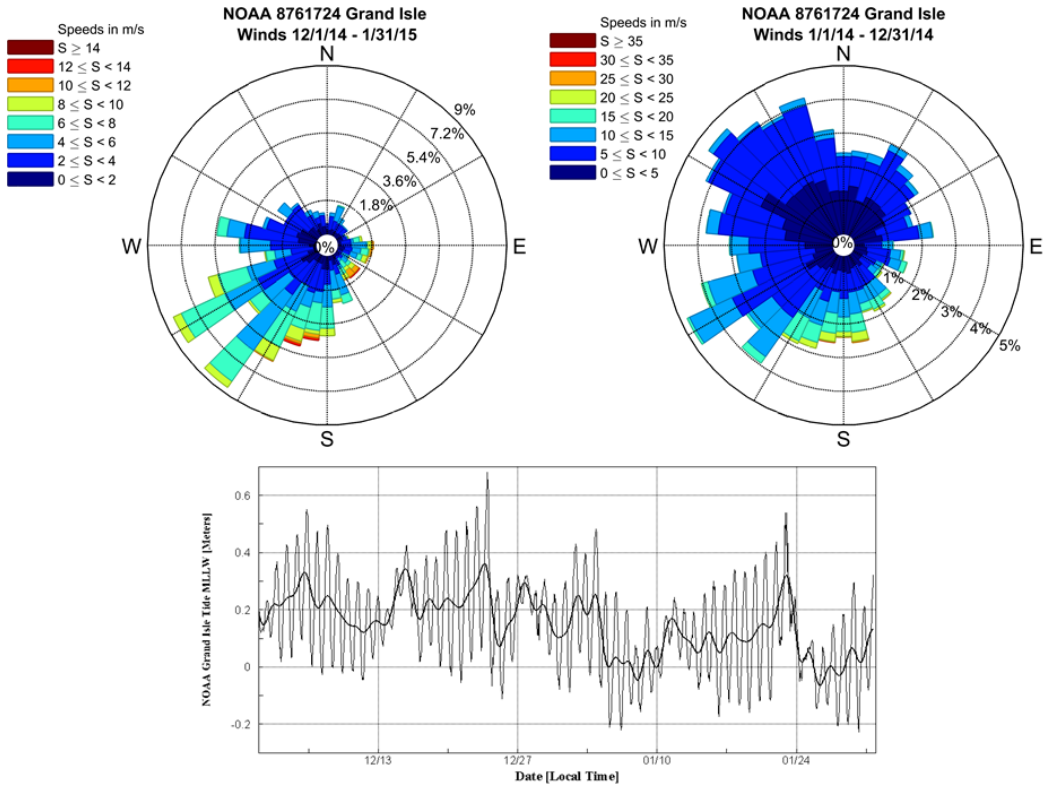

Figure 18: Windroses for the deployment period (top left), and the entire year (top right) and Grand Isle tidal variation during the deployment period (bottom). The thick black solid line for the Grand Isle tides shows the subtidal water variation using a low-pass filter with a 0.6 cycles per day cutoff frequency.

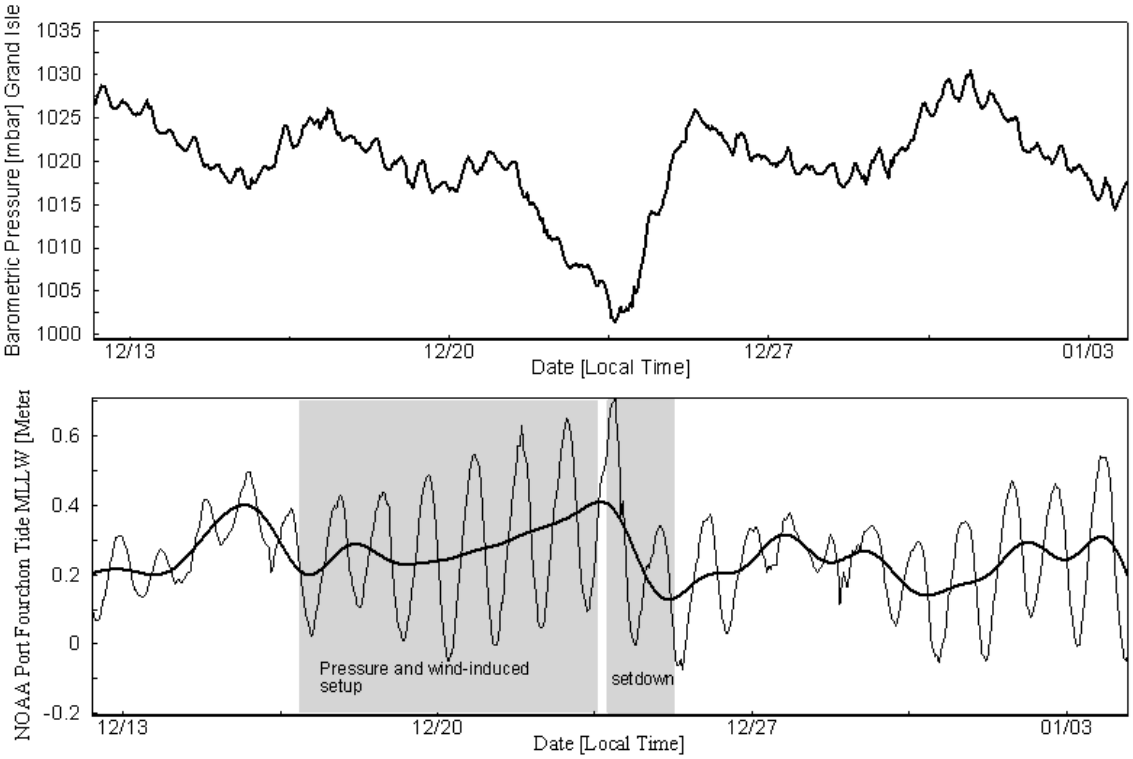

Figure 19: Barometric pressure (top) and tidal and sub-tidal water level variations at Port-Fourchon during the December 2015 storm (bottom). Grayed out sections of the water-level plot indicate the phases of bay set up and set down created by the pre and post frontal winds.

TIDAL INLET CURRENTS

Data collected by the deployment at Raccoon Pass and East Timbalier Pass exhibit (as expected) demonstrated bidirectional velocities (depth-averaged) ranging between -0.5 to 0.5 m/s (Figure 19). The punctuated effect of the storms caused the ebb velocity to increase by as much as 130%, whereas the flood velocity was decreased by as much as 20%. For instance, flood velocities are reduced to 0.4 m/s, whereas ebb velocities during storms increase to more than 1 m/s. And immediately following the storm, ebb velocities peak to 1.5 m/s. Tidal range leading to the storm increases as part of the astronomical forcing, whereas at the same time the system experiences sub-tidal increase (Figure 17, bottom). However, at the inlet (Figure 20, top) while tidal variations undergo a similar trend, the spring tide, as well as sub-tidal water response is suppressed leading to the peak of the storm; the tidal range immediately after the storm declines in a manner that is consistent with the tides recorded at Port Fourchon. Significant wave heights at Raccoon Pass (Figure 20, middle) range from 10-20 cm during non-storm conditions to in excess of 1.0 m during storms. The significant wave heights increased as the storm peaked, and decreased rapidly post storm as would be expected. Sub-tidal water flux, indicated by the low pass filter on the observed signal of the axial tidal velocity, shows a strong ebb response; the inlet initially experiences bi-directional velocity but became increasingly ebb dominant as the storm developed. At the peak of the storm, the inlet did not experience any flood velocity but rather is dominated by ebb flow.

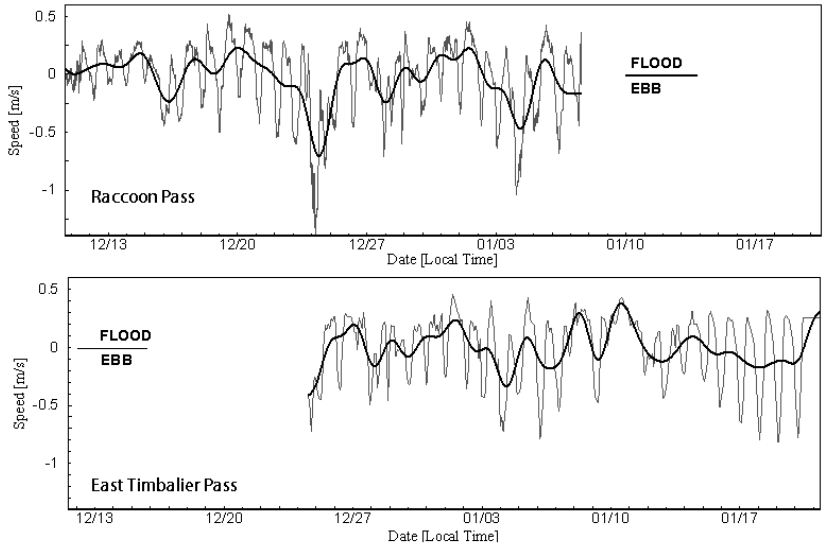

Figure 20: Axial velocities at Raccoon Pass (top) and East Timbalier Pass (bottom) during the deployment period.

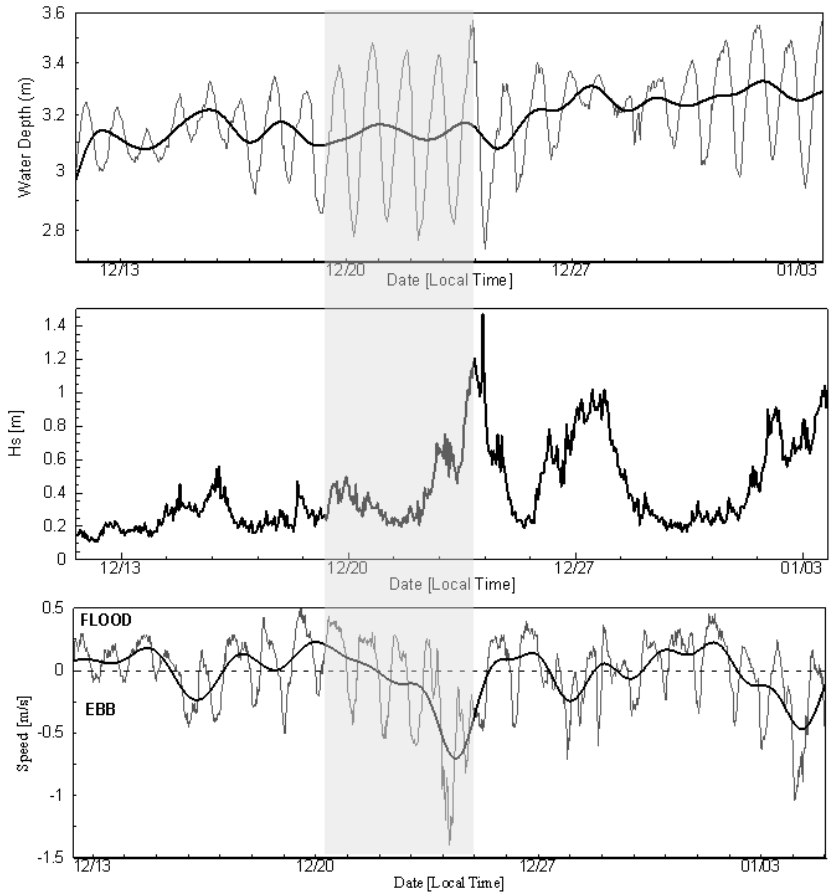

Figure 21: Tidal and sub-tidal water level variations at Raccoon Pass and significant wave height evolution (middle) and axial velocity with low pass filter (bottom) during the December 2015 storm (greyed out section).

Discussion

MORPHOLOGICAL EVOLUTION

The West Belle Pass Barrier Spit represents an immature flanking barrier influenced by the installation of hard structures, tidal inlet enlargement, and the occurrence of storms impacting the area. The results of this study clearly depict shoreline deterioration occurring down-drift of a jetty structure; however, hard structures are not the only cause of morphological change within the study area, and their influences are considered (i.e., an enlarging tidal inlet). Determining the exact cause of shoreline erosion and a particular event's role is difficult without more high resolution data documenting event based physics and resulting morphology. Nonetheless, the morphological evolution of the West Belle Pass Barrier Spit was most likely controlled by a reduction in the sediment input from up-drift littoral transport processes caused by the installation and extension of the jetties, along with gradual changes at the Raccoon Pass inlet facilitated by the ongoing transgression (i.e., increasing cross-sectional area, and thus sediment bypassing). Here, we present a historical interpretation of the evolution of the system, starting with the damming of Bayou Lafourche, since it is the earliest event influencing the study area. The evolution of the barrier system is discussed in two parts, which illustrate the main natural and anthropogenic events during their respective timeframes.

A. Early Influences (1904 – 1939)

While no published rates of littoral drift exist predating the damming of Bayou Lafourche in 1904, the closing of Bayou Lafourche likely had an effect on the study area. The damming of the bayou arguably signifies the end of fluvially transported sediment, which would have been a potential source of sediment for the area from outside the system. This means that longshore sediment transportation after 1904 (and possibly before) is perhaps the only long-term source of sediment for the West Belle Pass Barrier Spit. Dantin et al. (1978) calculated rates of shoreline erosion directly east and west of Belle Pass between 1885 and 1974. Of particular interest is the interval between 1885 and 1932, wherein upstream controls (e.g., damming of Bayou Lafourche) and storm impacts contributed to the deterioration of the study site. The shorelines directly east and west of Belle Pass experienced erosion rates of 21-35 m/yr between 1885 and 1932 (Dantin et al., 1978). The upper range of shoreline erosion (30-35 m/yr) occurred on the shoreline down-drift of Belle Pass. Dantin et al. (1978) argued that if most of the erosion during this period began in 1904, shoreline erosion rates increase to 35-58 m/yr for the 28-year period. Perhaps, one reason for the increased rates of erosion down-drift of the mouth of Bayou Lafourche is due to the damming at Donaldsonville, which deprived the study site of seasonal floodwater waters that supplied much needed sediment to the area. With a dominant wave approach from the southeast, it is possible that fluvial sediment would have been deposited near West Belle Pass Barrier and the surrounding shoreline. In addition to the damming of Bayou Lafourche, the unnamed 1915 category 3 hurricane likely played a role in shoreline erosion, effects that are accounted for in the Dantin et al.(1978) study. The degree to which this storm affected the study site is not detectable due to the time between subsequent datasets. Nevertheless, the preferential erosion occurring down-drift of Belle Pass between 1885 and 1932 marks the beginning of shoreline reorientation. The increased rates of erosion at the West Belle Pass Barrier caused the shoreline to transgress faster than the shoreline east of Belle Pass, and West Belle Pass Barrier exhibited slight clockwise rotation from 1884 to 1933 that was mainly due to natural causes.

B. Late Influences (1940 - 2013)

The West Belle Pass Barrier shoreline rotation was exacerbated by the completion of the Belle Pass jetties in 1940 and subsequent modifications. Although the jetties were completed in 1940, it seems that the initial construction (pre-modifications) was not enough to completely shut down sediment bypassing, evidenced by the lack of sediment accumulation on the up-drift (east) side of the jetties. The extension (over 2 km) of the West Belle Pass Barrier Spit suggests that sediment supply to this area from up-drift sources continues after 1940, although a contrasting argument may be that the sediment delivered herein, post jetty construction, may also be sourced from widespread shoreface erosion of the Caminada Headland. Yet, relative rates of supply are difficult to determine without additional study. Regardless, with the extension of the jetties in 1956, the sediment bypassing under day-to-day conditions is negligible, leaving bypassing on the middle and lower shoreface as the only up-drift (punctuated) sediment source for the area.

The most prominent morphological discrepancy between the shorelines immediately east and west of the Belle Pass jetties in 1956 was the shoreline strike. The two shoreline morphologies that predate jetty installation show a more or less uniform headland shoreline striking northeast to southwest. However, the 1956 shoreline dataset depicts a different orientation, particularly regarding the area directly west of the jetties. The shoreline strike of East Timbalier Island, the majority of West Belle Pass Barrier, and the shoreline of the Caminada-Moreau Headland exhibited the same strike orientation in 1956. Yet, the portion of shoreline immediately west (> 1 km) of the jetties was oriented northwest to southeast. This suggests that the jetties begun hindering sediment bypassing more significantly, and that any bypassing taking place was not nourishing the down-drift barrier directly. For example, sediment bypassing would likely be happening at depths in excess of 2-3 m given the depth of Belle Pass, hence the sediment likely bypasses seward of the West Belle Pass and is not available readily to nourish the barrier spit. Dantin et al. (1978) modeled the effect of the jetties for design purposes and not barrier morphology, but did document a change in the wave refraction patterns and resulting longshore transport rates as a result, which support to some extend our observations and statements using shoreline change analysis. Other mechanisms of down-drift erosion at the West Belle Pass may be that a significant fraction of the bypassing sediment volume (at depth) discussed previously through a punctuated processes (i.e., event based) is eventually bypassing the barrier altogether through Raccoon Pass. Evidence of this process in modern times (post 1930's) is the enlargement of Raccoon Pass to facilitate the exchange between Timbalier Bay, and in more recent time (post 2005) the growth of the West Belle Pass Spit and spit platform. List et al. (1984) shows that while erosion from 1880 to 1930 was widespread along this segment; erosion rates were uniform across the headland with massive shoreface erosion, and uniform landward migration. However, post 1930, List et al. (1984) document the growth of Raccoon Pass (a result of a 1965 storm) and the accompanied growth of the flood-tidal delta. During this period (1930-1980), there was likely a gradual geomorphic shift of the system toward one that supports barrier extension, diminishing of up-drift sediment supply, inlet breaching, and enlargement of the flood-tidal delta. Likely, these processes initiated and continue to support/facilitate the modern sediment transport trends in the area.

Miner et al. (2009) compared bathymetric change using BICM data (1930-1980) and re-did the analysis of List et al. (1984) to document approximately 1.0-3.0 m of accretion on the landward side of Raccoon

Pass in the shape of a flood-tidal delta. The backbarrier accretion and flood-tidal delta formation suggests that tidal currents were sufficient enough to transport sediment from the shoreface to the backbarrier, sometime between the 1930's and 1980's. Through correlations of seafloor change and shoreline change analysis with one timely hurricane impact, coupled with the construction and extension of the Belle Pass jetties created a system where sediment is being bypassed around the jetties and deposited outside the littoral zone, subsequently re-worked either onto the West Belle Pass barrier a few kilometers down-drift, or funneled into the backbarrier through the inlet and deposited on the flood-tidal delta. Continued barrier shoreline deterioration and rotation at the West Belle Pass Barrier during the 1980's, 1990's, and early 2000's, allowed for the continual sequestration of sediment at the flood-tide delta through Raccoon Pass. A conceptual model depicting this evolutionary model is shown in Figure 22.

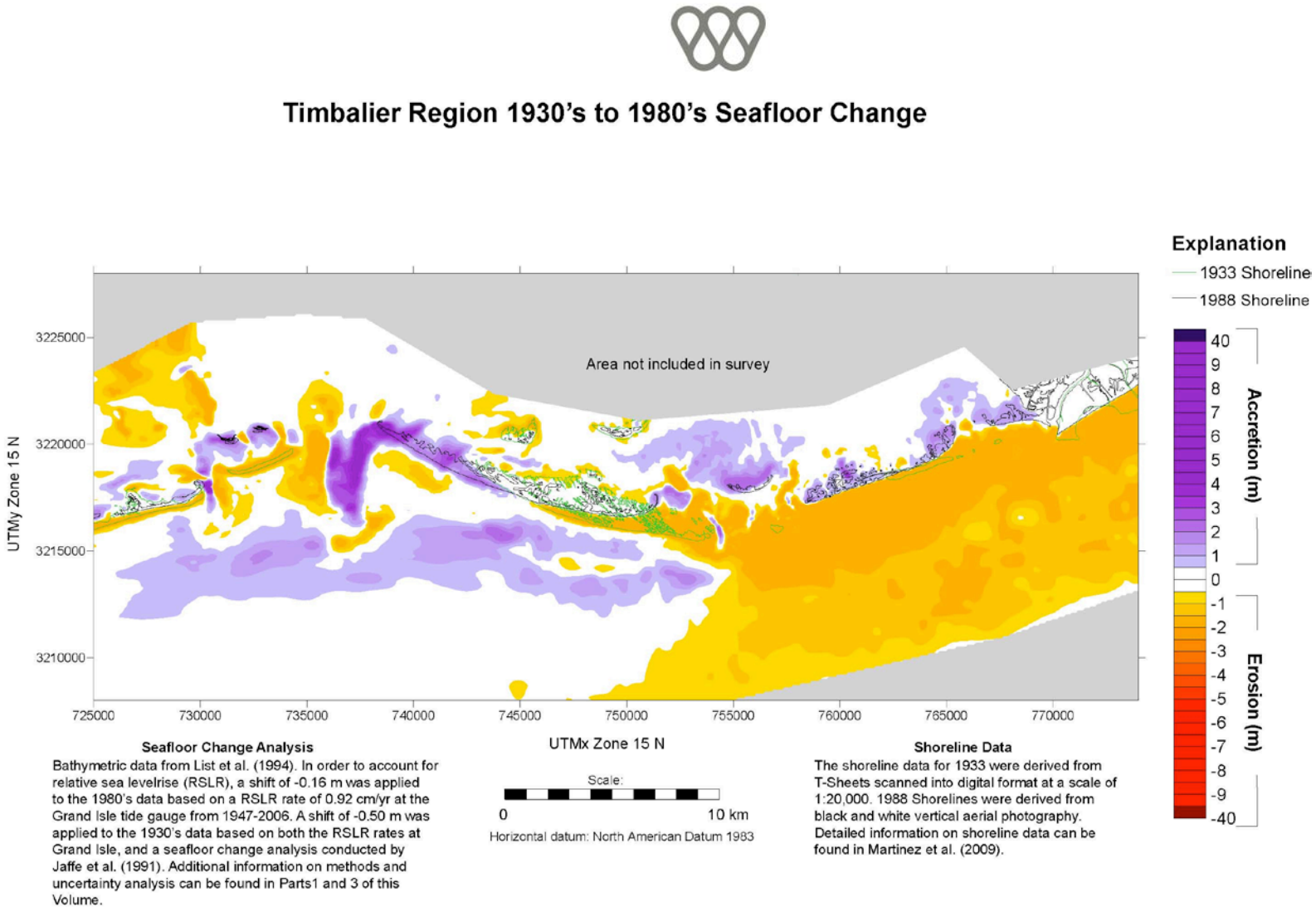

Figure 22: A 1930's to 1980's bathymetric change map of the region between the Isles Deneries and Caminada-Moreau Headland (Miner et al., 2009). During this time period, the back barrier environment of the West Belle Pass Barrier experienced approximately 1.0 to 3.0 m of net accretion (red box).

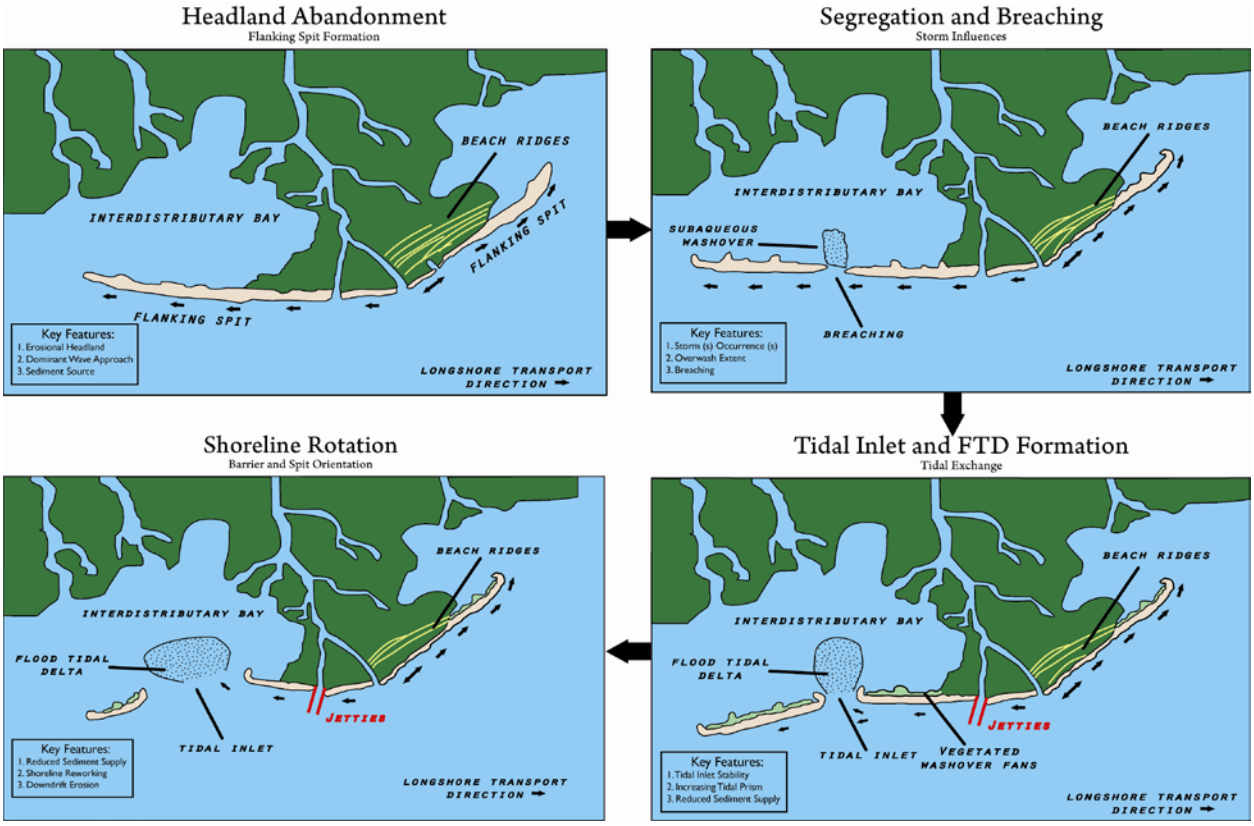

Figure 23: Conceptual model depicting the interplay of jetty construction, shoreline revetment, sediment supply and longshore sediment transport along the west side of the Caminada-Moreau Headland.

The tidal currents through Raccoon Pass, evidenced by the tidal current collected in this study, do have the capacity to transport fine sand, especially during energetic conditions. The enlargement of the tidal inlet at Raccoon Pass and East Timbalier Pass, was facilitated by interior wetland loss in the Terrebonne Basin, with documented an average rate of 24 km^2/yr from 1956 to 1978 (Barras et al., 1994), a rate that was the highest rate of land loss of all basins used in the study. The conversion of wetlands into open-water areas support increase of the tidal prism (FitzGerald et al., 2007) and can support faster water velocities and thus water and sediment fluxes during storms. However, the paucity of flood-tidal deltas along coastal Louisiana suggests that tidal currents alone are not responsible for the formation of the delta, and hence, the deterioration of the West Belle Pass Barrier. This suggest that a series of very unique and timely events surrounding the construction and extension of the Belle Pass jetties may have contributed to this quite unusual system, coupled with other revetment activities west near East Timbalier Island. A barrier that has limited up-drift sediment supply would undergo transgression and any onshore sediment transport would have to be sourced from the shoreface (Short, 1099). Typically, this takes place during larger less frequent storm events. Tidal analysis shows that the water level variations exhibit ebb dominance, with flood durations of 0.40-0.45 days, while ebb durations are 0.55-0.60 days, when influenced mostly by astronomical forcing (Figures 18 and 20). Tidal currents at the inlet throat (Figures 19 and 20) show a similar effect (i.e., ebb dominance) but display periods or pulses of flood dominance (Figure 20). FitzGerald et al (1983) showed that tidal asymmetries across tidal inlets do exist, and (at least) in semi-diurnal settings flood-dominance on the spit platform was documented despite the inlet throat being ebb dominant. However, this was not documented extensively in diurnal settings as tidal

asymmetries are strongly influence by among other things, the inlet morphology (Dronkers 2002; Fridrichs & Aubrey, 1998). However, in mixed or wave-dominated inlets such as Raccoon Pass, during storms, there is likely a change in the dominance, which could further support the role of storms in shaping the regional geomorphology. This periodic change in the dominance suggests that other, more frequent events such as cold fronts can produce conditions that support punctuated transport that can explain the regional geomorphology and provide insights into the mechanisms that explain regional sediment pathways within the backbarrier basin.

Conclusion

Historical shoreline analysis and stratigraphic cross section interpretation through vibracore analysis were used to evaluate the morphological changes within the West Belle Pass Barrier spit, the tidal inlet complex at Raccoon Pass and the associated flood tidal delta. The morphological evolution of West Belle Pass Barrier (and more recently barrier spit) was influenced largely by the installation and extension of the Belle Pass jetties coupled with an expanding tidal inlet complex at Raccoon Pass as part of the ongoing transgression of the Caminada Headland. While the specific causes for the expansion of the tidal inlet complex at Raccoon Pass are not clear, a likely initiation of the expansion can be attributed to Hurricane Betsy in 1965. The tidal inlet complex continued expansion can be explained by the gradual reduction is sediment bypassing from updrift sources (e.g. Caminada) and the slow shift from downdrift bypassing toward East Timbalier Island to sediment bypassing to backbarrier environments. The bypassing mechanism in this system appears to have changed over the last 70 years, from one where lateral migration driven by more abundant sediment transport volumes with significant inlet bypassing, to the modern system where transport volumes are far less abundant and little bypassing, with the exception of sediment that is now routed to the backbarrier. Sediment bypassing to the backbarrier is further influenced by the armoring of the East Timbalier Island shoreline which halted the retreat of the island and caused in place drowning. If East Timbalier Island was migrating according to historical rates (pre-1956) as the rest of the coast, backbarrier transport or backbarrier bypassing would not be so pronounced. Modern hydrodynamic observations and analysis demonstrate that while the inlet is ebb dominant as expected, during winter storms the inlet quickly become flood dominant with swift currents and waves proximal to the inlet that contribute to asymmetric sediment transport trends. While such deposits do not have direct benefits to downdrift barriers and at first may appear to hinder the morhodynamics of the coupled inlet barrier flood-delta complex, deposits as such (eg flood tidal delta) may serve as future sediment sources as the barrier complex migrates landward as part of the continued transgression. Moreover, what used to be a flood tidal delta associated with a previous shoreline now outcrops onto the shoreface and likely contributes sand to the littoral zone. This outlier behavior is not directly transferable to other regions of the Louisiana Coastal Zone, but highlights an important aspect of sediment availability and a unique approach to evaluate future sediment dynamics and deposits within the barrier complex and proximal environments, where punctuated sediment transport can be enhanced when these deposits are intercepted during transgression.

References

Brown, E.I. 1928. Inlets on Sandy Coasts: Proceedings of the American Society of Civil Engineers, v. 54, no. 4, p. 505 – 553.

Coleman, J.M. 1988. Dynamic Changes and Processes in the Mississippi River Delta Plain: *Geological Society of America Bulletin*, v. 100, p. 999 - 1015.

Condrey, R. Kemp, P., Visser, J., Gosselink, J., Lindstedt, D., Melancon, E., Peterson G., and Thompson B. 1995. Status, trends and probable causes of change in living resources in the Barataria and Terrebonne estuarine systems: BTNEP Publ. No. 21, Barataria Terrebonne National Estuary Program, Thibodeaux, Louisiana, 434 pp.

Dantin, E.J., Whitehurst, C.A., and Durbin, W.T. 1978. Littoral drift and erosion at Belle Pass, Louisiana: Journal of the Waterway, Port, Coastal and Ocean Division, Proceedings of the American Society of Civil Engineers, v. 104, no. WW4, p. 375-390.

Davis, R.A., Jr., and Fitzgerald, D.M., 2004, Beaches and Coasts: Blackwell. Oxford, UK, 419p.

Escoffier, F.F., 1940, The Stability of Tidal Inlets: Shore and Beach. v. 8, no. 4, p. 114–115.

Evans, O.F., 1942, The Origin of Spits, Bars, and Related Structures: *Journal of Geology*, v. 50, p. 846 – 863.

Fisk, H.N., 1952, Geological Investigation of the Atchafalaya Basin and the Problem of the Mississippi River Diversion. Vicksburg, MS: US Army Corps Eng.

Fisk H.N., and McFarlan E. 1955. Late Quaternary Deltaic Deposits of the Mississippi River. Spec. Pap. 62, p. 279 – 302, *Geological Society of America*, Boulder, CO.

Fitzgerald, D.M., 2005, Tidal Inlets: in Schwartz, M. L. (ed.), Encyclopedia of Coastal Science: Springer, Dordrecht, The Netherlands, p. 958–964.

Fitzgerald, D.M., Kulp, M. A., Penland, S., Flocks, J., and Kindinger, J., 2004, Morphologic and Stratigraphic Evolution of Muddy Ebb-Tidal Deltas Along a Subsiding Coast: Barataria Bay, Mississippi River Delta: Sedimentology, v. 51, p. 1157–1178.

Frazier, D. E. 1967. Recent Deltaic Deposits of the Mississippi River: Their Development and Chronology. *Gulf Coast Association of Geological Societies Transaction*s, v. 17, p. 287-315.

Georgiou, I.Y., Fitzgerald, D.M., and Stone, G.W. 2005. The Impact of Physical Processes along the Louisiana Coast, *Journal of Coastal Research*, Special Edition No. 44, p. 72-89.

Georgiou, I.Y., Weathers, H.D., Kulp, M.A., Miner, M., and Reed, D.J. 2010. Interpretation of Regional Sediment Transport Pathways using Subsurface Geologic Data. Submitted to the US Army Corps of Engineers, CESU Contract # W912HX-09-0027.

Harper, J. R. 1977. Sediment Dispersal Trends of the Caminada-Moreau Beach-Ridge System: Gulf Coast Association of Geological Societies Transactions, v. 27, p. 283-289.

Hayes, M.O., 1975, Morophology of Sand Accumulation in Estuaries: in Cronin, L.E., (ed.), Estuarine Research: New York, Academic Press, p. 3-22.

Hoyt, J.H. and Henry, V.J., Jr., 1967, Influence of Island Migration on Barrier-Island Sedimentation: Geological Society of America Bulletin, v.78, p. 77-86.

Kosters, E.C., and Suter, J.R., 1993, Facies relationships and systems tracts in the Late Holocene Mississippi Delta Plain. J. Sediment. Res. v. 63, p. 727-733

Kulp, M.A., Fitzgerald, D.M., Penland, S., Motti, J., Brown, M., Flocks, J., Miner, M., McCarthy, P., and Mobley, C., 2006, Stratigraphic Architecture of a Transgressive Tidal Inlet-Flood Tidal Delta System:Raccoon Pass, Louisiana: Journal of Coastal Research, SI 39, p. 1731–1736.

List, J.H., Jaffe, B.E., Sallenger, A.H., Jr. Williams, S.J., McBride, R.A., and Penland, S., 1994, Louisiana Barrier Island Erosion Study: Atlas of Seafloor Changes from 1878 to 1989: Reston, Virginia, U.S. Geological Survey and Louisiana State University, Miscellaneous Investigations Series I-2150-A, 81 p.

List, J.F., Jaffe, B.E., Sallenger, A.H., and Hansen, M.E., 1997, Bathymetric Comparisons Adjacent to the Louisiana Barrier Islands: Processes of Large-Scale Change: Journal of Coastal Research, v. 13, p. 670–678.

Lombardo, J.S., 1992, The Geology of East Timbalier Island, Louisiana; an Aerial and Surficial Investigation. M.S. Thesis. University of Southwestern Louisiana, Lafayette, LA. 154 pp.

Martinez, L., Penland, S., Fearnley, S., O'Brien, S., Bethel, M., and Guarisco, P., 2009, Louisiana Barrier Island Comprehensive Monitoring Program (BICM), Vol. 2, Shoreline Change Analysis: 1800s to 2005: University of New Orleans, Pontchartrain Institute for Environmental Sciences Technical Report.

Matias, A., et al. "Classification Of Washover Dynamics In Barrier Islands." Geomorphology 97.3-4 (2008): 655-674. GeoRef. Web. 4 Nov. 2013.

Miller G.B., 1994, Coastal Habitat Restoration Planning in Louisiana: Lessons from the Greenhill-Timbalier Bay Oil Spill Case. Coastal Management, v. 22, p. 413-420.

Miner, M.D., Fitzgerald, D.M., and Kulp, M.A., 2007, 1880 to 2005 Morphologic Evolution of a Transgressive Tidal Inlet, Little Pass Timbalier, Louisiana: in Proceedings, Coastal Sediments 07, New Orleans, American Society of Civil Engineers, p. 1165–1178.

Miner, M.D., Kulp, M., Flocks, J., Twichell, D., Penland, S., Martinez, L., Motti, J., Weathers, H.D., DeWitt, N., Reynolds, B.J., Baldwin, W., Danforth, B., Worley, C., Bergeron, E., Ferina, N., McCarthy, P., Brown, M., and Torres, J., 2009a, Louisiana Barrier Island Comprehensive Monitoring Program (BICM), Vol. 3, South-Central Louisiana ans Northern Chandeleur Islands, Bathymetry and Historical Seafloor Change 1873-2006, Part 1: Methods and Error Analysis for Bathymetry: University of New Orleans, Pontchartrain Institute for Environmental Sciences and U.S. Geological Survey, Submitted to Louisiana Department of Natural Resources, 44 p.

Miner, M.D., Kulp, M., Flocks, J., Twichell, D., Penland, S., Martinez, L., Motti, J., Weathers, H.D., DeWitt, N., Reynolds, B.J., Baldwin, W., Danforth, B., Worley, C., Bergeron, E., Ferina, N., McCarthy, P., Brown, M., and Torres, J., 2009b, Louisiana Barrier Island Comprehensive Monitoring Program (BICM), Vol. 3, South-Central Louisiana ans Northern Chandeleur Islands, Bathymetry and Historical Seafloor Change 1873-2006, Part 2: South-Central Louisiana and Northern Chandeleur Islands, Bathymetry Maps: University of New Orleans, Pontchartrain Institute for Environmental Sciences and U.S. Geological Survey, Submitted to Louisiana Department of Natural Resources, 27 p.

Miner, M.D., Kulp, M.A., Fitzgerald, D.M., and Georgiou, I.Y., 2009c, Hurricane-Associated Ebb-Tidal Delta Sediment Dynamics: Geology, v. 37, no. 9, p. 851-854

Miner, M.D., Kulp, M.A., Fitzgerald, D.M., Flocks, J.G., Weathers, H.D., 2009d, Delta Lobe Degradation and Hurricane Impacts Governing Large Scale Coastal Behavior, South-Central Louisiana, USA: Geo-Marine Letters, v. 29, no. 5 – 6

Morgan, J.P., and Larimore, P.B., 1957. Change in the Louisiana Shoreline. Transactions of the Gulf Coast Association of Geological Societies, v. 7, p. 303-310.

Mossa, J., Penland, S., and Moslow, T.F.. 1985. Coastal structures in Louisiana's Barataria Blight: Coastal Geology Technical Report, Baton Rouge, Louisiana Geological Survey, n. 1, 28 p.

Otvos, E. G. Jr. 1969. A Subrecent Beach Ridge Complex in Southeastern Louisiana. Geological Society of America Bulletin, v. 80, p. 2353-2357.

Parker, P., Sweeney, R., and Linder, C., 2012, Louisiana Barrier Island/Headland Restoration – Two Ongoing Projects' Lessons Learned and Construction Comparison: U.S. Department of Commerce, National Oceanic and Atmospheric Administration, NOAA Fisheries, Powerpoint Presentation, 51 slides.

R. Pawlowicz, B. Beardsley, and S. Lentz, 2002. Classical tidal harmonic analysis including error estimates in MATLAB using T_TIDE, Computers and Geosciences 28 (2002), 929-937.

Penland, S., Boyd, R., Nummedal, D., and Roberts, H., 1981. Deltaic barrier development on the Louisiana coast. Supplement to Transactions, Gulf Coast Association of Geological Societies, v. 31, p. 471-476.

Penland, S. & Boyd, R.. 1985. Transgressive Depositional Environments of the Mississippi River Delta Plain: Louisiana Geological Guidebook Series No. 3. p. 233.

Penland, S., Ritchie, W., Boyd, R., Gerdes, R. G., and Sutter, J. R., 1986. The Bayou Lafourche delta, Mississippi River delta plain, Louisiana: Geological Society of America Centennial Field Guide – Southeastern Section, p. 447-452.

Penland, S. and Suter. J.R. ,1988. Barrier Island Erosion and Protection in Louisiana: A coastal Geomorphological Perspective: Gulf Coast Association of Geological Societies Transactions v. 38, p. 331-342.

Penland, S., Suter, J. R., and Boyd, R.. 1985. Barrier Island arcs along abandoned Mississippi River deltas. Marine Geology. v. 63, p. 197-233.

Peyronnin, C. A., Jr. 1962. Erosion of the Isles Dernieres and Timbalier Islands: Journal of the Waterways and Harbors Division, American Society of Civil Engineers, v. 88, p. 57-69.

Reed, D., ed. 1995. Status and Trends of Hydrologic Modification, Reduction in Sediment Availability, and Habitat Loss/Modification in the Barataria-Terrebonne Estuarine System. Barataria-Terrebonne National Estuary Program, Thibodaux, LA, 20: 388 pp.

Short, A.D. 1999. Handbook of Beach and Shoreface Morphodynamics. Wiley and Sons, Chichester.

THE WATER INSTITUTE
OF THE GULF®

301 NORTH MAIN STREET, SUITE 2000
BATON ROUGE, LA 70825

(225) 448-2813
WWW.THEWATERINSTITUTE.ORG